Int. J. Heat Mass Transfer. Vol. 34, No. 11, pp. 2837–2857, 1991
Printed in Great Britain

0017–9310/91 $3.00+0.00
Pergamon Press plc

Heat and mass transfer in pressure-gradient boundary layers

B. A. KADER
Institute of Atmospheric Physics, U.S.S.R. Academy of Sciences, Pyzhevsky 3, Moscow, 109017, U.S.S.R.

(*Received* 12 *December* 1988)

Abstract—The structure of a scalar field (temperature or concentration of some passive admixture) in moving-equilibrium boundary layers with longitudinal pressure gradients is studied by the dimensional analysis and asymptotic expansion method. It follows from the analysis that a self-similar region named the 'gradient sublayer' (where the mean temperature distribution is described by the inverse half-power law) exists in both decelerating and accelerating pressure-gradient wall flows. Moreover, the temperature defect law of special form is valid in the outer zone of strong gradient boundary layers. The available experimental data on temperature profiles in decelerating wall flows permit one to determine universal constants and functions entering into the theoretical relationships and to obtain interpolation formulae describing the mean temperature field under such conditions. Assuming that an overlap layer exists, where both the defect law and gradient-sublayer law are valid, one can obtain the universal heat and mass transfer law. The numerical coefficients of this law are estimated for decelerating pressure-gradient flows. The forms of some statistical characteristics of temperature fluctuations (in particular, the multidimensional probability density, spectra and moments) in the gradient sublayer are found by dimensional analysis and compared with the available experimental data.

1. INTRODUCTION

UNLIKE the study of the dynamic structure of pressure-gradient turbulent flows that have evoked a fairly large number of contributions, the study of heat and mass transfer in such flows has received relatively little attention despite the great engineering importance of these processes. This is mainly explained by great experimental difficulties encountered in the study of heat and mass transfer. It is clear that the longitudinal pressure gradient introduces an additional complexity into the experimental investigation of the mean temperature field and of its turbulent fluctuations. Therefore, it is no surprise that the available literature contains very few experimental results suitable for verifying the conclusions presented below. Note also that almost all these results relate to heat transfer in air flows which are characterized by a nearly constant Prandtl number ($Pr \cong 0.7$).

The lack of necessary experimental data also explains the meagreness of theoretical works dealing with the temperature or concentration field in a pressure-gradient turbulent flow. Here, among the most important works are the papers by Perry *et al.* [1], who, using dimensional considerations, obtained 'the inverse square root law' for the mean temperature profile in a zone of pressure-gradient boundary layer, and by Afzal [2], where the method of matched asymptotic expansions was applied to derive the same law. Both these papers used the same experimental data from ref. [1] related to the air boundary layer on a plate; therefore, the possible effect of Prandtl number on the temperature profile and heat transfer law were not tackled in these studies.

In the present paper the general analysis of the problem of heat and mass transfer in pressure-gradient wall flows will be given. It will be assumed that $Pr \gtrsim 0.7$. This means that the case of heat transfer in liquid metals, where $Pr \ll 1$, will not be considered here (since there are no experimental data to verify the theoretical conclusions related to such a transfer).

Only the two-dimensional turbulent flow of an incompressible fluid will be considered below, and it will be assumed that the substance transferred is dynamically passive, i.e. it does not influence the velocity field. Moreover, it will be supposed that for both the velocity field U and the temperature (or concentration) field T the hypothesis about the moving equilibrium is satisfied with an adequate accuracy. This hypothesis states that, at a given value of the longitudinal coordinate x, all characteristics of these fields depend only on the values of the external flow parameters at the same value of x (see ref. [3] dealing with the mean velocity field and friction law for pressure-gradient flows). It should be noted at the outset that the validity of this hypothesis for the velocity field does not automatically entail the same for the temperature and concentration fields. Therefore, the condition $U_0/(\gamma\delta)^{1/2} \gg 1$ (where U_0 is the velocity at the outer edge of the boundary layer of thickness δ, $\gamma = \rho^{-1}|\mathrm{d}P/\mathrm{d}x|$ the kinematic pressure gradient, and ρ the density), which was stated in ref. [3] as the approximate condition guaranteeing the validity of the moving-equilibrium hypothesis for the mean velocity field, is a necessary one but not sufficient for the flows studied in this paper. Indeed, certain restrictions should also be imposed on the boundary conditions for the T field; in particular, a very sharp variation

NOMENCLATURE

a thermal diffusivity
a_i universal constants
c_p specific heat at constant pressure
c_f skin friction coefficient
$E_{\theta\theta}$, $E_{\theta v}$ temperature spectrum and temperature and velocity cospectra
F_θ flatness factor of temperature fluctuations
H thickness of thermal boundary layer
K_i universal constants
k wave number
N temperature dissipation
P_θ probability density of temperature fluctuation distribution
$\mathrm{d}P/\mathrm{d}x$ longitudinal pressure gradient
Pr thermal or diffusion Prandtl number
Q temperature flux
q heat flux
R_i longitudinal correlation functions
r argument of longitudinal correlation functions
S $\delta_p/\delta_v = u_*^3/\gamma\nu$
S_θ asymmetry of temperature fluctuations
St Stanton number
T mean temperature
t_* friction temperature, Q/u_*
U mean longitudinal velocity
u, v, w longitudinal, normal to the wall and transverse velocity fluctuations, respectively
u_* friction velocity
x, y, z longitudinal, vertical and transverse coordinates, respectively
y_+, ξ, η dimensionless vertical coordinates, $y/\delta_v, y/\delta_p, y/\delta$
Z $\delta/\delta_p = \gamma\delta/u_*^2$.

Greek symbols
α_i universal constants
$\beta(Pr)$ function of Pr entering into equation (8a)
Γ_θ function in equation (14)
γ kinematic pressure gradient, $\rho^{-1}|\mathrm{d}P/\mathrm{d}x|$
Δ thickness of molecular heat transfer sublayer
δ_K, δ_θ Kolmogorov and temperature microscales of turbulence
$\delta_v, \delta_h, \delta_p$ viscosity, heat transfer and pressure-gradient length scales, respectively, $\nu/u_*, a/u_*, u_*^2/\gamma$
ε_h coefficient of eddy diffusion of heat
θ temperature fluctuations
ρ density
τ time
ϕ_i, ψ_i universal functions.

Subscripts
θ temperature field
$+$ dimensionless quantities
o conditions at the outer edge of the boundary layer
p pressure-gradient quantities
w wall.

Superscripts
θ refers to temperature field
p gradient quantities.

of the wall temperature T_w will make the structure of the temperature field dependent on $\mathrm{d}T_w/\mathrm{d}x$, i.e. it will lead to the inapplicability of the moving-equilibrium hypothesis for the temperature field even in the constant-pressure case.

2. MEAN TEMPERATURE PROFILE AND HEAT TRANSFER IN PRESSURE-GRADIENT FLOWS

2.1. *Theoretical analysis*

Since there are no experimental data on mass transfer in pressure-gradient boundary layers, only heat transfer will be discussed below, bearing in mind, however, that the results can also be applied to mass transfer after evident change of notation.

In addition to dimensional parameters that were listed in ref. [3] as relevant for the description of the kinematic characteristics of the moving-equilibrium pressure-gradient boundary layer (i.e. the parameters γ, δ, the kinematic viscosity coefficient ν, and the friction velocity u_*), it is now necessary to add the temperature flux $Q = q_w/c_p\rho$ (where q_w is the wall heat flux and c_p the heat capacity) or 'friction temperature' $t_* = Q/u_*$, as well as the thermal boundary layer thickness H and thermal diffusivity $a = \nu/Pr$.

An attempt will be made to determine, at least roughly, what conditions guarantee the applicability of the moving-equilibrium hypothesis to the mean temperature field in a pressure-gradient flow. For simplicity, only the effect of the longitudinal pressure gradient on the thermal boundary layer will be considered which develops on the plate under the conditions where the variations of all the parameters different from P along the coordinate x are negligible. The characteristic time τ_c of the longitudinal variation in the velocity U_o of the incident flow, which entails the variation in the structure of both the dynamic and thermal boundary layers with x, is equal to $|\mathrm{d}U/\mathrm{d}x|^{-1} = U_o/\gamma$. The temperature relaxation time

τ_r is determined by the quantities Q, H, u_* and by the temperature difference $T_w - T_o$ between the wall and the incident flow. Therefore, $\tau_r \sim QH/u_*^2(T_w - T_o)$. Since the dimensionless intensity of heat transfer—the Stanton number—is defined as $St = Q/U_o(T_w - T_o)$ while $(u_*/U_o)^2 = c_f/2$, it is obtained that

$$\tau_r \sim \frac{St}{c_f/2}\frac{H}{U_o}.$$

But the validity of the inequality $\tau_r \ll \tau_c$ is clearly necessary for the applicability of the moving-equilibrium hypothesis to the temperature field. Hence the condition

$$\frac{c_f/2}{St}\frac{U_o^2}{\gamma H} \gg 1 \qquad (1)$$

is necessary for the possibility to use the moving-equilibrium approximation in this paper. In the case of a sharp change in the wall boundary conditions (when the derivatives dT_w/dx or dq_w/dx can no longer be regarded as small), it is necessary to check whether the logarithmic derivatives satisfy the inequalities

$$\frac{d[\ln (T_w - T_o)]}{d(x/H)} \ll 1 \quad \text{or} \quad \frac{d(\ln Q)}{d(x/H)} \ll 1. \qquad (2)$$

Under conditions (1) and (2), it is possible to assume that the temperature profile of the pressure-gradient wall flow is determined by the values of five length scales: the thicknesses of the viscous and molecular heat transfer $\delta_v = \nu/u_*$ and $\delta_h = a/u_*$, the pressure-gradient length scale $\delta_p = u_*^2/\gamma$, the thicknesses of the dynamic and thermal boundary layers δ, and H. Thus, it follows from the dimensional analysis that the temperature profile is described by the function of five dimensionless arguments and can be represented by three equivalent expressions

$$\frac{\partial T}{\partial y} = \frac{Q}{\nu}\psi_1^{(p)}\left(\frac{yu_*}{\nu}, \frac{u_*^3}{\gamma\nu}, \frac{\delta u_*}{\nu}, \frac{\delta}{H}, Pr\right)$$
$$= \frac{Q\gamma}{u_*^3}\psi_2^{(p)}\left(\frac{y\gamma}{u_*^2}, \frac{\gamma\nu}{u_*^3}, \frac{\delta u_*}{\nu}, \frac{\delta}{H}, Pr\right)$$
$$= \frac{Q}{\gamma^{1/2}H^{3/2}}\psi_3^{(p)}\left(\frac{y}{H}, \frac{\gamma\delta}{u_*^2}, \frac{\delta u_*}{\nu}, \frac{\delta}{H}, Pr\right). \qquad (3)$$

Determination of the form of these functions from experimental data seems to be unreal. However, the above formulae can be substantially simplified in special flow zones where some arguments of the functions $\psi_i^{(p)}$ take on very large or very small values. Assuming that the corresponding limits exist, one can simply replace, in the first approximation, the small argument by zero and the large by infinity. First, consideration will be given to the gradient flow with length scales satisfying the conditions

$$\max(\delta_v, \delta_h) \ll \delta_p \ll \min(\delta, H)$$

(cf. schematic (Fig. 1)). The validity of the above inequalities means that the turbulent boundary layer is developed dynamically and thermally so that $Re_* = \delta/\delta_v = \delta u_*/\nu \gg 1$ and $Pe_* = H/\delta_h = Hu_*/a \gg 1$. Then it can be expected that the flow is self-similar with respect to Re_* and Pe_* and the argument $\delta u_*/\nu$ in equation (3) can be replaced by infinity, i.e. can be ignored.

Now simplifications of equations (3) will be considered which can be used in some special zones of the turbulent boundary layer.

When $0 \ll y \ll \delta_p$ (and, therefore, also when $y \ll \min(\delta, H)$) the scales δ_p, δ, and H should not affect the structure of the thermal boundary layer and, consequently, the temperature profile is described here by the ordinary law of the wall

$$\partial T/\partial y = (Q/\nu)\psi_1^{(p)}(y_+, Pr), \quad T_+(y) = \phi_1^{(p)}(y_+, Pr),$$
$$T_+(y) = [T_w - T(y)]/t_*, \quad y_+ = y/\delta_v = yu_*/\nu \qquad (4)$$

which follows from the first line of equation (3) when $S = \delta_p/\delta_v = u_*^3/\gamma\nu \to \infty$ and when the dependence on δ/H is neglected. In the zone of the validity of equation (4), the longitudinal pressure gradient, just as the flow type, exerts no effect on the flow, i.e. here the temperature profile is the same as that in constant-pressure flows. In the case of large pressure gradients, when the ratio $S = \delta_p/\delta_v$ or $\delta_p/\delta_h = S \cdot Pr$ is not very large any longer, the quantity S enters into the list of wall law arguments, so that

$$\partial T/\partial y = (Q/\nu)\psi_1^{(p)}(y_+, S, Pr),$$
$$T_+(y) = \phi_1^{(p)}(y_+, S, Pr). \qquad (4a)$$

The quantities ν, a, δ, H are not important within the range of y values satisfying the inequalities $\max(\delta_v, \delta_h) \ll y \ll \min(\delta, H)$ (see again Fig. 1). Hence here the gradient law of the following form is valid:

$$\partial T/\partial y = (Q\gamma/u_*^3)\psi_2^{(p)}(\xi), \quad \xi = y/\delta_p = y\gamma/u_*^2. \qquad (5)$$

Note that the function $\psi_2^{(p)}$ must be the same for different types of flow (for the boundary layer on a plate, diverging or converging ducts of any cross-section and so on). However, for not very large values of $Z = \delta/\delta_p = \gamma\delta/u_*^2$, this argument must also be preserved in the second line of equation (3) and therefore

$$\partial T/\partial y = (Q\gamma/u_*^3)\psi_2^{(p)}(\xi, Z). \qquad (5a)$$

If the longitudinal pressure gradient is so large that δ_p is of the same order of magnitude as $\max(\delta_v, \delta_h)$ (but the condition $Z \gg 1$ is also fulfilled by virtue of the requirement that the turbulence must be developed), then for $y \ll \min(\delta, H)$

$$\partial T/\partial y = (Q\gamma/u_*^3)\psi_2^{(p)}(\xi, S, Pr). \qquad (5b)$$

In the outer region of the boundary layer where $y \gg u_*^2/\gamma$ and $y \gg \max(\delta_v, \delta_h)$, the temperature defect law must be valid

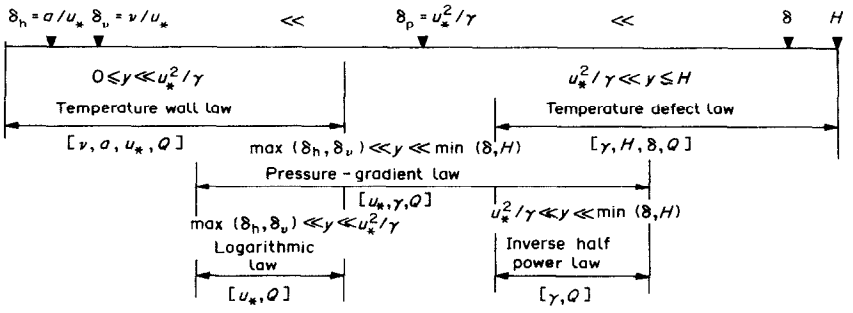

FIG. 1. The scheme of the validity range of similarity laws for the temperature field in the developed turbulent boundary layer with a longitudinal pressure gradient. The dimensional parameters of the problem which define the flow in the region under consideration are indicated in square brackets.

$$\frac{\partial T}{\partial y} = \frac{Q}{\gamma^{1/2} H^{3/2}} \psi_3^{(p)}\left(\eta, \frac{\delta}{H}\right),$$

$$\frac{T(y) - T_0}{Q/\sqrt{(\gamma H)}} = \phi_3^{(p)}\left(\eta, \frac{\delta}{H}\right), \quad \eta = \frac{y}{H}. \tag{6}$$

This law follows from the dimensionality arguments and from the assumption about the existence of

$$\lim_{Z \to 0, Re_* \to \infty} \psi_3^{(p)}(\eta, Z, Re_*) = \psi_3^{(p)}(\eta, 0, \infty)$$

where $\psi_3^{(p)}$ is the function entering into the third line of equation (3). Thus, as it is noted in Fig. 1, in this region the friction velocity u_* falls out of the list of relevant dimensional parameters. This falling out is due to the condition $y\gamma/u_*^2 \gg 1$ which determines the outer zone of the thermal boundary layer. It is clear that the condition $y\gamma/u_*^2 \to \infty$ is equivalent to $u_* \to 0$. At the same time, the temperature flux Q, which is also related to the boundary conditions on the wall, keeps affecting the temperature profile in this flow region. The reasons given above also imply the conclusion that the physical properties of the fluid have no effect on the profile $T(y)$ in the flow zone considered, but this profile can depend on the type of flow.

In the case of weak pressure-gradient flows it can be expected that the temperature defect law includes the function of three arguments

$$\frac{\partial T}{\partial y} = \frac{Q}{\gamma^{1/2} H^{3/2}} \psi_3^{(p)}\left(\eta, Z, \frac{\delta}{H}\right),$$

$$\frac{T(y) - T_0}{Q/\sqrt{(\gamma H)}} = \phi_3^{(p)}\left(\eta, Z, \frac{\delta}{H}\right). \tag{6a}$$

It seems clear, at first sight, that in the case when the dynamic and thermal boundary layers start at the same point $x = 0$, the ratio δ/H must take a constant (and, besides, fairly close to unity) value, so that the argument δ/H can be simply discarded in all the previous formulae. This question, however, needs a more detailed consideration, which is given in Appendix A. It is explained there that it is reasonable to use the definition of the thickness H which eliminates the effect of the molecular transfer sublayer on H. Such a definition leads to the equations

$$T_+(H) = 0.99 T_{0+} + 0.01\beta(Pr),$$
$$\beta(Pr) = (3.85 Pr^{1/3} - 1.3)^2 + 2.12 \ln Pr \tag{7}$$

which determine the value of H, and for this H the assumption made above turns out to be valid, i.e. the ratio δ/H actually becomes constant for constant-pressure flows.

The situation is much more complex for flows with strong pressure gradients. Here the hydrodynamic structure of the outer part of the boundary layer becomes independent at all of the magnitudes of the wall momentum flux (i.e. of friction velocity) and is determined by the longitudinal pressure gradient alone, while the temperature profile in this zone is kept substantially dependent on the wall heat flux Q.

Obviously, the strong turbulent mixing in the outer zone of the decelerating turbulent boundary layer considerably decreases the variation of the temperature profile with y in this region and hence also decreases the thickness H, whereas strong negative pressure gradients suppress the turbulent mixing in this region of the boundary layer and hence produce the strong dependence of $T(y)$ on y and the increase of H.

The formulae given above for the temperature profile in different zones of the pressure-gradient boundary layer are much simpler than general equations (3), but they also contain some unknown functions of several variables which must be found either from experimental data or from some approximate semi-empirical theories. More definite conclusions can be obtained assuming that there exist overlapping regions of the asymptotic expansions stated above, where two different asymptotic representations of the temperature field are simultaneously valid. Thus, assuming that there exists the zone, $\max(\delta_\nu, \delta_h) \ll y \ll \delta_p$, of matching the wall and gradient laws, it is easy to find that

$$(yu_*/Q)\partial T/\partial y = y_+ \psi_1^{(p)}(y_+, Pr)$$
$$= \xi \psi_2^{(p)}(\xi) = -\alpha = \text{const}. \tag{8}$$

Therefore, the temperature profile is described in this zone by the logarithmic equations

$$T_+(y) = \alpha \ln y_+ + \beta(Pr) \tag{8a}$$

$$T_+(y) = \alpha \ln \xi + \beta_2(Pr, S), \quad \beta_2 = \beta(Pr) + \alpha \ln S. \tag{8b}$$

The values of the universal constant α and of the function $\beta(Pr)$ (which is determined by the temperature difference between the wall and the lower edge of the logarithmic sublayer) must not differ from the corresponding values in constant-pressure flows. Hence, according to ref. [4], $\alpha = 2.12$, whereas the function $\beta(Pr)$ is given by equation (7). Thus, the logarithmic law of the temperature distribution appears to be valid in a certain region of distances from the wall also in the pressure-gradient non-isothermal flows with not too strong pressure gradients.

Equation (4), which for $y_+ \lesssim 4Pr^{-1/3}$ has the linear form $T_+(y) = Pr\, y_+$ and for $y_+ \gg 1$ has logarithmic asymptotic (8a), can be approximated by a single interpolating formula, e.g. by the formula suggested in ref. [5], namely:

$$T_+(y) = Pr\, y_+ \exp(-G) + [2.12 \ln(1+y_+) + \beta(Pr)] \exp(-1/G)$$

where $G = 10^{-2}(Pr\, y_+)^4/(1+5Pr^3\, y_+)$.

In the zone of the overlapping of the gradient law, equation (5), and the temperature defect law, equation (6), where $u_*^2/\gamma \ll y \ll \min(\delta, H)$, the following equation must hold:

$$(\gamma^{1/2} y^{3/2}/Q)\partial T/\partial y = \xi^{3/2}\psi_2^{(p)}(\xi) = \eta^{3/2}\psi_3^{(p)}(\eta) = -(1/2)K_1^{(\theta)} = \text{const.} \tag{9}$$

where the factor $-1/2$ is included for the convenience of subsequent integration. Thus, the matching of both these laws yields the formulae

$$[T_w - T(y)]/t_* = -K_1^{(\theta)}/\sqrt{\xi} + K_2^{(\theta)}(S, Pr) \tag{9a}$$

$$[T(y) - T_o]/Q(\gamma H)^{-1/2} = K_1^{(\theta)}/\sqrt{\eta} + K_3^{(\theta)} \tag{9b}$$

which can naturally be called the 'inverse hall power law'.

Law (9a) was apparently first formulated in ref. [1] but there $K_1^{(\theta)}$, just as α in equation (8), was regarded to be dependent on the physical properties of the fluid (that is on Pr). Reference [1] also contains some experimental data on temperature profiles in the pressure-gradient non-isothermal air flow above a plate that confirmed the existence of a sublayer in which the temperature distribution obeyed relations (9). Based on these data, the authors recommended to take $K_1^{(\theta)}$ to be equal to 2.8 for any values of the adverse pressure gradient at $Pr = 0.7$. Afterwards this 'elegant' law was pretty well forgotten and, within the knowledge of the present author, it has not been discussed and used in the subsequent literature devoted to heat transfer in pressure-gradient flows, until ref. [2] appeared where equation (9a) was deduced by the asymptotic expansion method.

2.2. *Analysis of experimental results*

To verify the inverse half-power law, use will be made of the experimental data given in ref. [6]. Besides the convenience of processing these data (all experimental results are presented in the form of detailed tables), the data are also attractive since they provide the possibility of independent verification of the relations given above (note that the law under discussion is not mentioned in ref. [6]). In Figs. 2 and 3 these experimental data on temperature distribution in the equilibrium (in the sense that the dimensionless longitudinal pressure gradient $(2\nu/U_o^2)\, dU_o/dx$ remains constant along the plate) accelerating and decelerating flows are given as $T_+ = [T_w - T(y)]/t_*$ vs $(y\gamma/u_*^2)^{-1/2}$, i.e. in such a form that the law being verified is represented by a simple linear relation. For convenience, the thicknesses of the molecular sublayer ($y/\delta_h = Pr\, y_+ \cong y_+ = 30$) and of the near-wall zone of the boundary layer ($y/\delta = 0.1$) are also shown in the figures by dashed lines. The figures confirm the above theoretical reasonings by indicating that the inverse half-power law for the temperature profile is valid over a considerable portion, not only of the decelerating but also, the accelerating turbulent layer within a wide range of regime parameters. At the same time, the experimental data analysed do not agree well with the hypothesis about the constant value of $K_1^{(\theta)}$ independent of the magnitude of the longitudinal pressure gradient. Therefore, following the method suggested in ref. [3], use will be made here of a more general (than equation (9)) relation

$$[T_w - T(y)]/t_* = -K_1^{(\theta)}(Z)/\sqrt{\xi} + K_2^{(\theta)}(Z, S, Pr) \tag{9c}$$

$$[T(y) - T_o]/Q(\gamma H)^{-1/2} = K_1^{(\theta)}(Z)/\sqrt{\eta} + K_3^{(\theta)}(Z) \tag{9d}$$

where $K_1^{(\theta)}$ varies with Z for not too large values of Z.

The main difficulty of such an analysis is the insufficiency of the available empirical material summed up, for convenience, in Table 1. This pertains especially to accelerating flows. The data available for these flows make an impression that the main purpose of the authors of experimental works was to study the limiting case of the turbulent boundary layer relaminarization disregarding the case of moderate negative pressure gradients. Therefore, consideration will be given to the behaviour of $K_1^{(\theta)}(Z)$ only for decelerating boundary layers with a decrease in heat transfer.

First, an attempt will be made to evaluate the asymptotic behaviour of this function at small values of Z from the requirement of a smooth (up to the first derivative) matching of the logarithmic law, equation (8a), and inverse half-power law, equation (9a), at a certain point $y = y_1$. Naturally, this requirement is based on the assumption that the sublayer dividing the boundary layer regions, for which the two laws

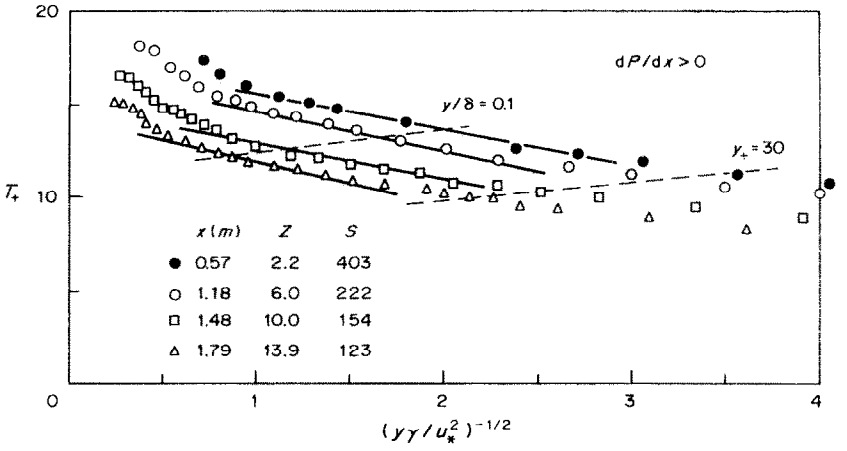

FIG. 2. Verification of the fulfillment of the inverse half-power law for the temperature profile in the wall zone of a decelerated boundary layer (according to the data of ref. [6]).

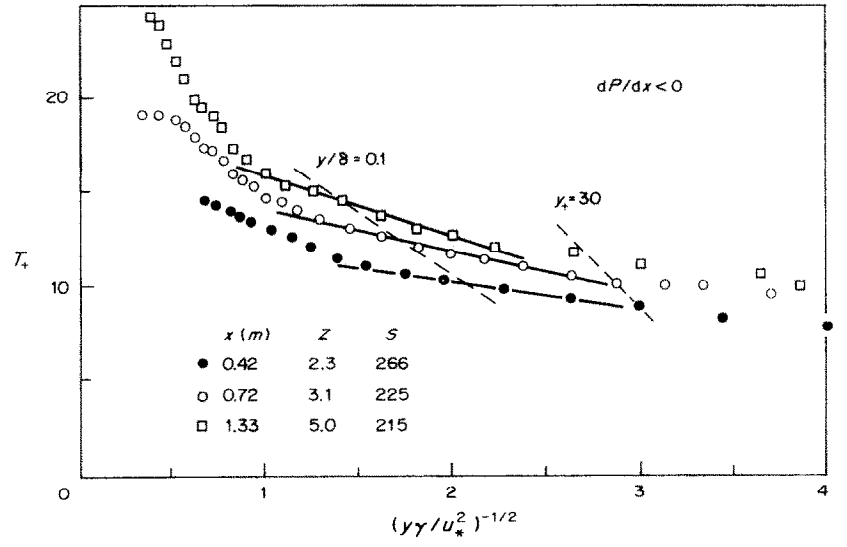

FIG. 3. Verification of the fulfillment of the inverse half-power law for the temperature profile in the wall zone of an accelerating boundary layer (according to the data of ref. [6]).

are valid, is very thin; therefore the results thus obtained are only approximate (however, it seems natural to hope that their accuracy will suffice for practical applications). Based on the assumption adopted, the conclusion can be drawn that $K_1^{(\theta)} = 2\alpha(y_1/\delta)^{1/2}Z^{1/2}$ when $Z \ll 1$. But since the lower limit of the validity zone for this law must not differ greatly from the upper limit of the logarithmic sublayer, where equation (8) is apparently valid, $y_1 \cong 0.15\delta$. Hence, taking $\alpha = 2.12$, it is easy to obtain that

$$K_1^{(\theta)} \cong 1.5Z^{1/2} \quad \text{when} \quad Z \ll 1. \tag{10}$$

On the other hand, the aforegoing dimensional considerations imply that in strongly gradient flows (for $Z \gg 1$) the function $K_1^{(\theta)}$ must tend to the universal constant dependent neither on the flow type, nor on physical properties of the fluid. Unfortunately, at present there are no experimental data which allow a complete verification of the latter theoretical prediction—all the experiments collected in Table 1 relate to air flows with $Pr \cong 0.7$. Nevertheless the available data cover a fairly wide range of Z values (namely, $1.5 \leqslant Z \leqslant 50$) which makes it possible to check the character of the dependence of $K_1^{(\theta)}(Z)$ on Z.

The data in Fig. 4 are rather scattered but on the whole they show that for the decelerating flows

$$K_1^{(\theta)} \cong 3 \quad \text{for} \quad Z \gg 1. \tag{11}$$

Moreover, the $K_1^{(\theta)}$ values appear to be close to the limiting value already at the values of $Z = \gamma\delta/u_*^2$ slightly above 10, while, according to the experimental results analyzed in ref. [3], a similar limit for the

Table 1. Summary table of experimental studies of the temperature field in two-dimensional decelerating and accelerating turbulent boundary layers on a plate

No.	Notation	Reference	Characteristics of the boundary layer			Notes
			dP/dx	$S=\delta_p/\delta_v=u_*^3/\gamma\nu$	$Z=\delta/\delta_p=\gamma\delta/u_*^2$	
1	2	3	4	5	6	7
1	○	[1]	>0	106–32	10.7–36	
2	—	[6]	<0	266–215	2.3–5.0	A2 experiment
	■		>0	403–123	2.2–13.9	A3 experiment
	◪		$>0,<0,>0$	392–48	1.4–21	A part of A5 experiment for $dP/dx>0$
	◧		$>0,<0,>0$	280–48	2.3–14.7	A part of A6 experiment for $dP/dx>0$
3	—	[19]	<0	73–31	8–14	Flow relaminarization
4	▽	[7]	>0	38–31	45–48	Points of origination of hydrodynamic and thermal boundary layers do not coincide
5	—	[39]	<0	88–63	12–13.8	Flow relaminarization
6		[11]	$<0,>0$	32–836	0.7–14.8	For the part of experimental data with $dP/dx>0$ succeeding the strong gradient, which, apparently, causes flow relaminarization

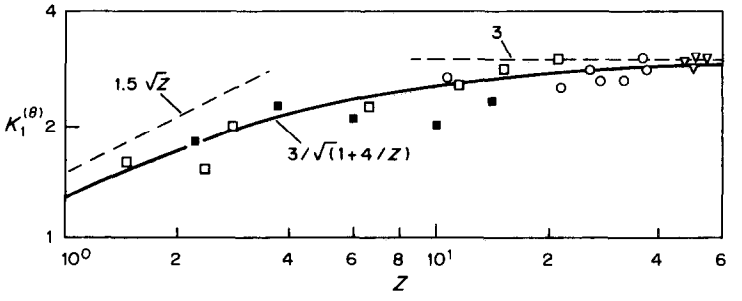

FIG. 4. The coefficient $K_1^{(\theta)}$ vs the parameter Z in the law (9c) and (9d) by the data of measurements for decelerated boundary layers. See notation in Table 1. The solid line corresponds to interpolation equation (12) and the dashed lines correspond to limiting relations (10) and (11).

function $K_1(Z)$ in the half-power law for the velocity profile is only reached when $Z \gtrsim 100$.

Based on the limiting relations (10) and (11), the following interpolating formula can be given

$$K_1^{(\theta)} = 3/\sqrt{(1+4/Z)}. \qquad (12)$$

This formula agrees rather well with all experimental points in Fig. 4 and has correct asymptotic behaviour at large and small values of Z.

The value $K_1^{(\theta)} = 2.8$, constant at all values of Z, was suggested in ref. [1] on the basis of the experiment performed and also in ref. [2] where the same experimental data were analysed. This value agrees well with the experimental results in Fig. 4 for $Z > 10$ but differs appreciably (almost by a factor of two) from the experimental points for low values of Z.

The same experimental data on the temperature profiles in decelerating turbulent wall flows allow one to estimate the additive function in equation (9a). For this it is sufficient, for instance, to plot the experimental data in the coordinates T_+, $(y\gamma/u_*^2)^{-1/2}$, as it was done in determining $K_1^{(\theta)}$ in Figs. 2 and 3, and to calculate the mean value of the sum $T_+ + K_1^{(\theta)}\xi^{-1/2}$ (where $K_1^{(\theta)}(Z)$ is determined from equation (12)) for all the points within the validity range of the inverse half-power law. It is clear that the thus obtained $K_2^{(\theta)}$ value corresponds to the segment cut off on the T_+ axis by the straight line drawn through the experimental point with the slope determined by relation (12).

For a rough theoretical estimation of the form of the function $K_2^{(\theta)}(S, Z, Pr)$ use will be made again of the simplest assumption about a smooth matching of the temperature profiles in the logarithmic sublayer and in the validity range of relation (9c) at $y = y_2$. This yields

$$y_2/\delta \cong (K_1^{(\theta)}/2\alpha)^2/Z$$

$$\text{and} \quad K_2^{(\theta)} \cong \alpha \ln \Gamma_\theta + \beta(Pr) + 2\alpha \qquad (13)$$

so that in this approximation $K_2^{(\theta)}$ appears to be dependent only on the Prandtl number and on the following special combination of S and Z:

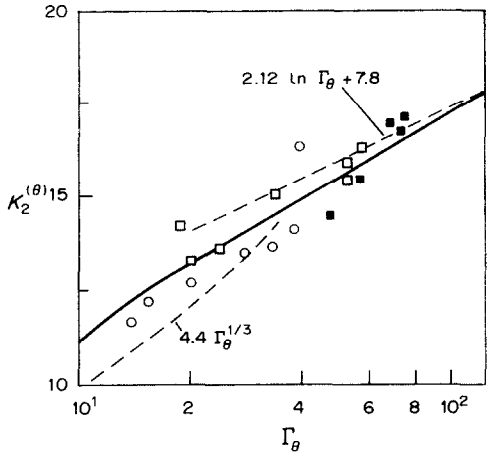

FIG. 5. The coefficient $K_2^{(\theta)}$ vs the values of the parameter Γ_θ in law (9c). The solid line corresponds to interpolation equation (18) and the dashed lines correspond to limiting relations (17).

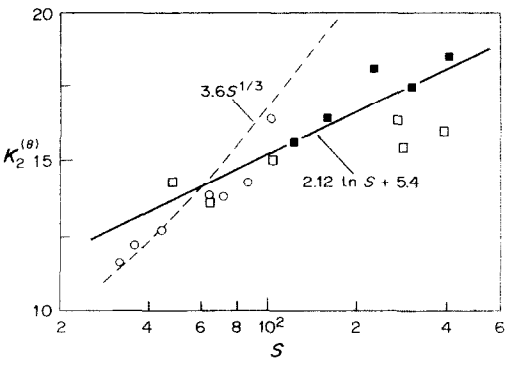

FIG. 6. The coefficient $K_2^{(\theta)}$ vs the parameter S in law (9c). The dashed line corresponds to the power law approximation of $K_2^{(\theta)}(S)$ for near separation flows. For notation see Table 1.

$$\Gamma_\theta = \left(\frac{K_1^{(\theta)}}{2\alpha}\right)^2 S = \frac{SZ}{2(4+Z)}. \tag{14}$$

It should be noted that $\Gamma_\theta \to S/2$ when $Z \to \infty$. Thus, in this case $K_2^{(\theta)}$ ceases to depend on Z and, in accordance with equation (9a), it is determined by the values of Pr and S. Besides, it follows from equation (13) that

$$K_2^{(\theta)} \cong \alpha \ln S + \beta(Pr) + (2+\ln 2)\alpha \quad \text{for} \quad Z \gg 1. \tag{15}$$

Equation (13) can be employed to estimate the function $K_2^{(\theta)}$ only in the case of large S, when there exists (see Fig. 1) a noticeable layer characterized by the logarithmic temperature distribution. At insufficiently large values of S such a layer can be absent; at small values of S one already observes the matching of the temperature profile described by the inverse half-power law with the linear distribution $T_+ = Pr\, y_+$ of the mean temperature in the molecular heat condition layer. In this case

$$y_3/\delta \cong (K_1^{(\theta)} S/2Pr)^{2/3} Z^{-1}$$

$$\text{and} \quad K_2^{(\theta)} = 3(\alpha\, Pr\, \Gamma_\theta)^{1/3}. \tag{16}$$

Thus, it can be concluded that

$$K_2^{(\theta)} = \begin{cases} 2.12 \ln \Gamma_\theta + \beta(Pr) + \text{const.} & \text{when } \Gamma_\theta \gg 1 \\ 5 Pr^{1/3}\, \Gamma_\theta^{1/3} & \text{when } \Gamma_\theta \gg 1 \end{cases}. \tag{17}$$

The experimental data that were obtained for the dependence of $K_2^{(\theta)}$ on Γ_θ for turbulent wall air flows ($Pr \cong 0.7$) by the above method are compared with the limiting relations in Fig. 5. The first of the limiting relations (17) agrees well with the experimental results for $\Gamma_\theta > 30$, if the additive constant in it is taken to be equal to 4 (it will be recalled that, according to equation (7), $\beta(0.7) = 3.8$). Note that this value agrees surprisingly well with the rough estimate of this constant which follows from equations (13), namely $2\alpha \cong 4$. The experimental data pertaining to the validity range of the second limiting relation (17) are not available in the literature, but, as can be seen from Fig. 5, when $\Gamma_\theta < 30$, the experimental points begin to depart appreciably downwards from the dashed curve which corresponds to a logarithmic relation (13). A comparatively good approximation of the entire experimental material available is given by the interpolating formula

$$K_2^{(\theta)} = 5(Pr\, \Gamma_\theta)^{1/3} \exp(-Pr\, \Gamma_\theta) + (2.12 \ln \Gamma_\theta + \beta(Pr) + 4) \exp(-1/(Pr\, \Gamma_\theta)) \tag{18}$$

which agrees with both equations (17).

It is useful to compare the relations derived with the formulae suggested for $K_2^{(\theta)}$ in refs. [1, 2]. It was assumed in both these papers that $K_2^{(\theta)}$ depends only on S. As it was illustrated above, this is true only at rather large values of Z. The experimental data available in the literature are presented in the form of the values of $K_2^{(\theta)}(S)$ in Fig. 6. In this figure the power-law approximation $K_2^{(\theta)} = c \cdot S^{1/3}$ (suggested in ref. [1]) for the values of $K_2^{(\theta)}$ at large values of Z is also plotted for $c = 3.6$ which is the value of c given in ref. [2]. Of course, this approximation agrees fairly well with the above-indicated rather old experimental results, but deviates markedly from the experimental points corresponding to large values of S (i.e. to the cases of moderate pressure gradients). Logarithmic equation (15) appears to be more successful, when the value of the constant term added to $\beta(Pr)$ is taken to be equal to 1.6 in lieu of the estimated value $(2-\ln 2)\alpha \cong 2.8$. However, even in this case the scatter of the experimental points round the approximating curve is somewhat higher than that in Fig. 5. The authors of ref. [1] also preferred to use the logarithmic relation of form (15) for $K_2^{(\theta)}$, but with different coefficients: $K_2^{(\theta)} = 2.0 \ln S + 4.9$.

For a complete description of the temperature pro-

file in the decelerated turbulent boundary layers it is also necessary to use the temperature defect law for the profile in the outer zone of the boundary layer. The analysis of the data related to this law will be given below only for the case when the difference between the thickness of the hydrodynamic and thermal boundary layers is not significant. With the exception of the results given in ref. [7], all experimental data on heat transfer in decelerating flows collected in Table 1 satisfy this condition. According to the above results (see equations (6) and (6a)), if $\delta/H = \text{const.} = 1$, then for moderate values of Z

$$(T-T_o)/Q(\gamma\delta)^{-1/2} = \phi_3^{(p)}(\eta, Z) \tag{19}$$

or

$$(T-T_o)/t_* = Z^{-1/2}\phi_3^{(p)}(\eta, Z). \tag{19a}$$

At the same time, at small values of Z the function $\phi_3^{(p)}$ on the right-hand side of equation (19a) must be representable as $Z^{1/2}\cdot\phi_4(\eta)$ where ϕ_4 does not depend on Z, since only under this condition equation (19a) for $Z \to 0$ yields the known relation

$$(T-T_o)/t_* = \phi_4(\eta) \tag{20}$$

which must be valid for constant-pressure flows.

Based on the analogy with the velocity profile in the outer zone of a constant-pressure boundary layer, which can be rather accurately described by the Coles wake law [8], it seems reasonable to try to apply a similar law also to the temperature profile in this flow region. This attempt is based on the conclusion that the temperature distribution here does not depend on the value of the molecular Prandtl number. To approximate the wake function $w(\eta)$, use will be made of the Moses polynomial $w(\eta) = 6\eta^2 - 4\eta^3$ (see, for instance, ref. [9]). The resulting formula

$$(T-T_o)/t_* = -2.12\ln\eta + 0.75(2-6\eta^2+4\eta^3) \tag{21}$$

(see also ref. [10]) is compared with the experimental data in Fig. 7 which shows that it agrees satisfactorily with the data.

In the other limiting case of large values of Z it is also possible to try to describe the temperature distribution in the outer zone of the pressure-gradient boundary layer with the aid of the Coles wake law with the wake function represented by the Moses polynomial. Here the wake function describes the deviation of the temperature profile from that given by the inverse half-power law rather than by the logarithmic law (as it is in the case of the constant-pressure flow). Therefore, here equation (19) takes the form

$$(T-T_o)/Q(\gamma\delta)^{-1/2} = 3(\eta^{-1/2}-1) + A(2-6\eta^2+4\eta^3). \tag{22}$$

The value of the constant A in this formula can be determined by comparing equation (22) with the experimental data from ref. [1] for $Z \gtrsim 20$ presented in Fig. 8. A good approximation of these data by equation (22) is attained for $A = 3.5$.

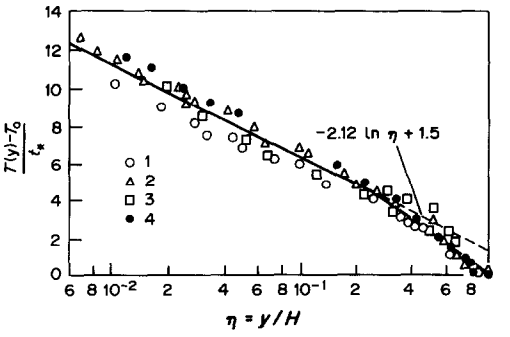

FIG. 7. The defect law for the temperature profile in the outer zone of a constant-pressure turbulent boundary layer on a plate. The solid line corresponds to equation (21) and the dashed line corresponds to the logarithmic asymptotics of the defect law. 1, 2, 3, refs. [19, 40, 41], for $Pr = 0.7$, 5 and 50, respectively; 4, ref. [18], $Pr = 0.7$.

It is also easy to set up the interpolating relation

$$\frac{T-T_o}{t_*} = -\frac{2.12}{1+Z}\ln\eta + \frac{3\sqrt{Z}}{1+Z}\left(\frac{1}{\sqrt{\eta}}-1\right) + \frac{15+3.5\sqrt{Z}}{20+Z}(2-6\eta^2+4\eta^3) \tag{23}$$

which has a correct asymptotic behaviour and agrees with all the results given above.

In conclusion, a list of formulae will be presented which permit one to calculate the temperature profile in decelerating turbulent boundary layers within a wide range of operational parameters and physical properties of the liquid, but which have been verified only for one value $Pr \cong 0.7$:

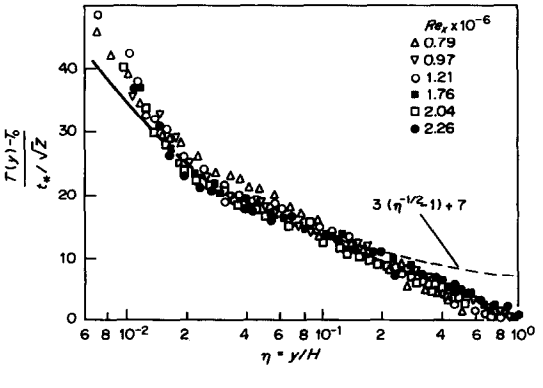

FIG. 8. The defect law for the temperature profile in turbulent boundary layers with a strong adverse pressure gradient. The solid line corresponds to the defect law, equation (22), at $A = 3.5$ and the dashed line corresponds to its asymptotics (to the inverse half-power law).

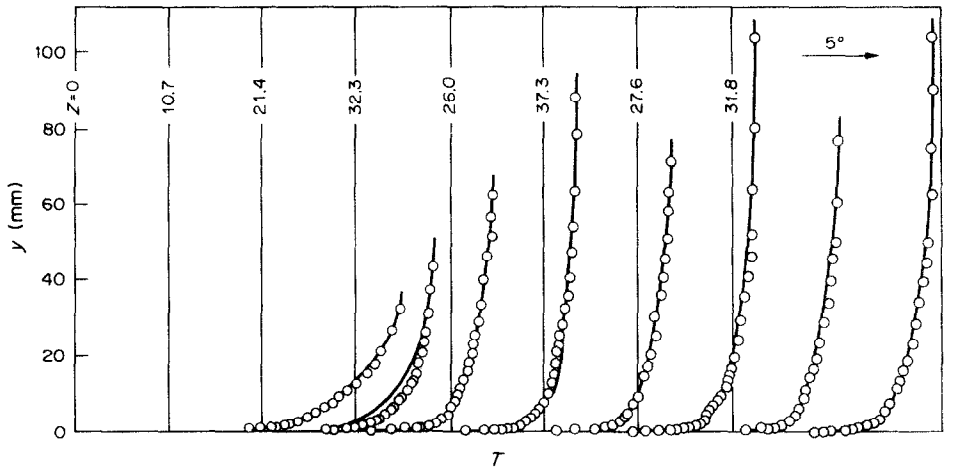

FIG. 9. Comparison of the measured (dots) and calculated (solid lines) temperature profiles on the basis of the data of ref. [1].

$$\frac{T_w - T(y)}{t_*} =$$

$$\begin{cases} Pr\, y_+ \exp(-G) + [2.12 \ln(1+y_+) + \beta(Pr)] \exp(-1/G) \\ \qquad \text{for } 0 \leqslant y_+ \leqslant y_1 u_*/\nu \qquad (24a) \\ -K_1^{(\theta)}/\sqrt{\xi} + K_2^{(\theta)} \\ \qquad \text{for } y_1\gamma/u_*^2 \leqslant \xi \leqslant y_2\gamma/u_*^2 \qquad (24b) \\ \dfrac{T_w - T_o}{t_*} + \dfrac{2.12}{1+z}\ln\eta - \dfrac{3\sqrt{Z}}{1+Z}\left(\dfrac{1}{\sqrt{\eta}} - 1\right) - \dfrac{15+3.5\sqrt{Z}}{20+Z}(2-6\eta^2+4\eta^3) \\ \qquad \text{for } y_2/H \leqslant \eta \leqslant 1. \qquad (24c) \end{cases}$$

Here $G = 10^{-2}(Pr\, y_+)^4/(1-5Pr^3\, y_+)$, $\beta(Pr) = (3.85 \times Pr^{1/3} - 1.3)^2 + 2.12 \ln Pr$, $(T_w - T_o)/t_* = (c_f/2)^{1/2}/St$, whereas $K_1^{(\theta)}$ and $K_2^{(\theta)}$ are given by equations (12) and (18), with y_1 being the ordinate of the intersection point of the wall law, equation (24a), and the inverse half-power law, equation (24b), and y_2 of laws (24b) and (24c). If the intersection points determining the values of y_1 and y_2 do not exist or $y_1 > y_2$, then the value of y_{12} is calculated, which corresponds to the intersection of the wall law (24a) with the temperature defect law (24c), and the temperature profile is approximated by the combination of these two relations.

Comparison of these formulae with the experimental data from refs. [1, 6] in Figs. 9 and 10 demonstrates the degree of accuracy of the given relations. The discrepancy does not exceed 5%, i.e. falls within the accuracy limits of the experiments under consideration. It is clear, however, that a complete verification of the suggested formulae requires experimental data on heat and mass transfer in decelerating wall flows with different physical properties to compare them with the data for gas flows.

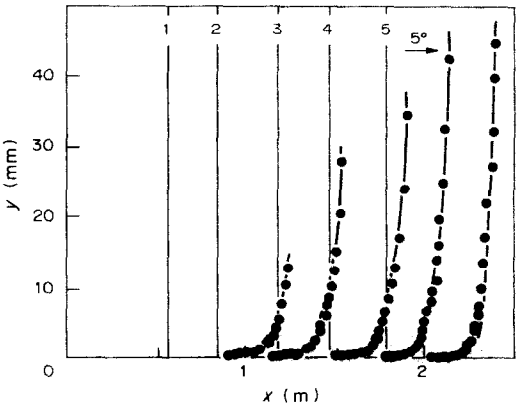

FIG. 10. Comparison of the measured (dots) and calculated (solid lines) temperature profiles based on the data of ref. [6].

2.3. *The universal law of heat and mass transfer in decelerating turbulent boundary layers*

A very attractive aspect of the scheme of reasoning used is the simplicity with which the general heat and mass transfer law can now be derived. For obtaining such a law, it suffices to sum equations (9c) and (9d) that represent the inverse half-power law (valid in the upper part of the gradient sublayer) and the temperature defect law (valid in the outer zone); in equation (9d), just as above, $Q(\gamma H)^{-1/2}$ on the left-hand side is replaced by $Q(\gamma\delta)^{-1/2}$, assuming that $\delta/H = \text{const.} \cong 1$. On making such a summation and taking the apparent equality $(T_w - T_o)/t_* = \sqrt{(c_f/2)}/St$ into account, one obtains

$$St = \frac{\sqrt{(c_f/2)}}{K_2^{(\theta)} + K_3^{(\theta)}/\sqrt{Z}}. \qquad (25)$$

This formula must be valid for both the accelerating and decelerating wall flows, but, as was demonstrated

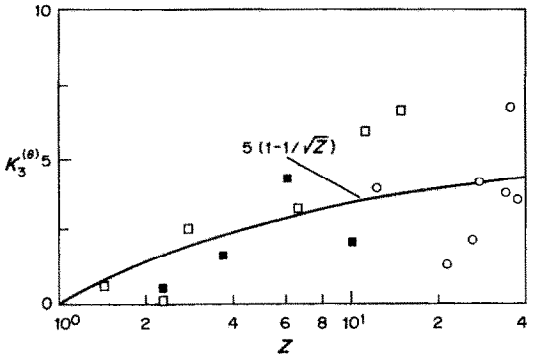

FIG. 11. The function $K_3^{(\theta)}(Z)$ in the heat transfer law, equation (25), for flows with an adverse pressure gradient. For notation see Table 1. The solid line corresponds to equation (26).

above, only for the latter case are there some experimental data which enable its verification.

For the case of a decelerating flow, the function $K_2^{(\theta)}$, entering into equation (25), can be approximately determined from equation (18): as regards $K_3^{(\theta)}$, this is the universal function of the parameter Z that appears in equation (9d) and which must tend to a constant for $Z \to \infty$ (see equation (9b)). The function $K_3^{(\theta)}$ can be estimated very roughly by assuming that the inverse half-power law (9d) is valid up to the upper edge of the thermal boundary layer ($\eta = 1$). This assumption results in $K_3^{(\theta)} = -K_1^{(\theta)}$, implying that for $Z \ll 1$, the function $K_3^{(\theta)}$ is proportional to $-Z^{-1/2}$, whereas, when $Z \to \infty$, it tends to the constant close to -3. According to the available experimental data given in Fig. 11, the experimental values of the function $K_3^{(\theta)}$ are very scattered which, of course, should have been expected, since $K_3^{(\theta)} = \sqrt{Z}[(T_w - T_o)/t_* - K_2^{(\theta)}]$ represents a small difference of large quantities which is multiplied additionally by a relatively large factor $\sqrt{Z}$. However, the latter circumstance also has a positive side, since, owing to it, even marked variations in $K_3^{(\theta)}$ exert only a slight effect on the predicted value of St. On the whole the data collected in Fig. 11 do not contradict the above conclusions about the form of the function $K_3^{(\theta)}(Z)$, except for the fact that, by these data, the limiting value of $K_3^{(\theta)}$ can never be negative for $Z \gg 1$. An acceptable approximation of the experimental data can be obtained, for instance, by setting

$$K_3^{(\theta)} = 5(1 - 1/\sqrt{Z}). \tag{26}$$

The predicted values of the dimensionless heat transfer coefficient, which are based on equations (18), (25) and (26), differ from the experimental values on the average by no more than 5%, whereas the maximum difference is of the order of 10%. The examples of a comparison of calculated and measured values of St are presented in Fig. 12.

Also of certain interest is the limiting form of the heat transfer law (25) for $\gamma \to \infty$. Here, when $\Gamma_\theta \to S/2$

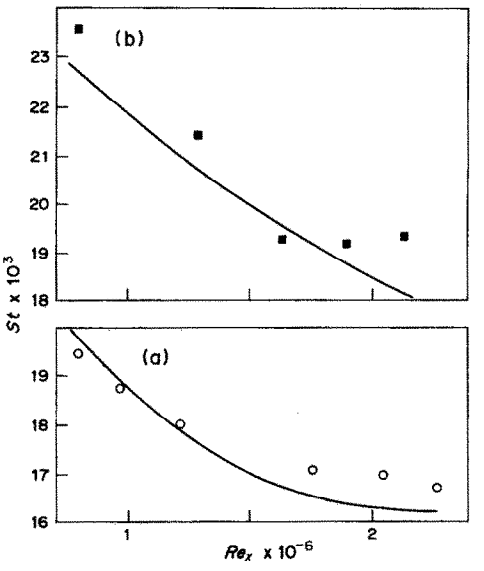

FIG. 12. Comparison of experimental (dots) and calculated (solid lines) values of the Stanton number on the basis of the experiments of ref. [1] (a) and of experiments of ref. [6] (b).

$$K_2^{(\theta)} \to 5((Pr\,S)/2)^{1/3} \exp((-Pr\,S)/2) + [2.12 \ln(S/2) + \beta(Pr) + 4] \exp(-2/(S\,Pr))$$

and $K_3^{(\theta)} \to 5$. Therefore, in this case

$$St^{-1} = (U_o/u_*)[K_2^{(\theta)} + K_3^{(\theta)}/\sqrt{Z}] \to 5U_o/\sqrt{(\gamma\delta)} + K_2^{(\theta)}\sqrt{(2/c_f)}.$$

Since $U_o/\sqrt{(\gamma\delta)} \cong 6.3$ at large Z (see equation (26) in ref. [3])

$$St^{-1} = 32 + \sqrt{(2/c_f)} \cdot K_2^{(\theta)}(S) \quad \text{for} \quad Z \gg 1. \tag{27}$$

When $Pr \gg 1$, with $\beta(Pr) \cong 14.8Pr^{2/3}$ starting to prevail in the expression for $K_2^{(\theta)}$, the above equation simplifies further to

$$St^{-1} = 14.8\sqrt{(2/c_f)}Pr^{2/3} \exp(-2/S) \quad \text{for} \quad Pr \gg 1$$

whereas when $S \gg 2$, it acquires the form of the following relation valid for constant-pressure flows:

$$St = 0.067 \cdot \sqrt{(c_f/2)}Pr^{-2/3}.$$

The only difference is that the value of the friction coefficient c_f for strongly decelerated wall flows appears to be much smaller than that for constant-pressure or weakly gradient flows.

It also follows from relation (27) that, for a fixed value of Pr (i.e. for instance, for heat transfer in gas flows), an increase of the adverse pressure gradient results in a decrease of the local heat transfer coefficients. At the same time, here the Reynolds analogy coefficient $St/(c_f/2)$ grows. Indeed, it is not difficult to infer from equation (27) that at large positive pressure gradients

$$St/(c_f/2) \cong 6.3\sqrt{Z}/K_2^{(\theta)}(S) \tag{28}$$

and, since $K_2^{(\theta)}$ changes here comparatively slowly (only logarithmically), the magnitude of the ratio in question increases rapidly

$$St/(c_f/2) \sim \sqrt{Z}$$

despite the decrease of St. This inference is in qualitative agreement with the experimental data of ref. [11] and with the approximate calculations given in ref. [12].

3. TEMPERATURE FLUCTUATIONS IN PRESSURE-GRADIENT BOUNDARY LAYERS

While the available literature contains some data on the temperature profiles in pressure-gradient turbulent flows, which are suitable for the verification of theoretical conclusions, there are almost no data on statistical characteristics of the scalar field (temperature or concentration) fluctuation in such flows. Therefore, the forthcoming theoretical conclusions mostly take the form of predictions, which can be compared with some data only to a very small degree.

(1) Based on the moving-equilibrium hypothesis which was discussed above (see also ref. [3]) and, moreover, assuming that

$$\max(\delta_v, \delta_h) \ll \delta_p \ll \min(\delta, H)$$

(see Fig. 1), one can formulate the corollaries which follow from the application of the general dimensional arguments to the simultaneous multi-dimensional probability density of the normalized temperature (θ/t_* or $\theta\sqrt{(\gamma H)}/Q$) and velocity ($\mathbf{u}/u_*$ or $\mathbf{u}/\sqrt{(\gamma\delta)}$) fluctuations at arbitrary n flow points $\mathbf{X}_1 = (x_1, y_1, z_1), \ldots, \mathbf{X}_n = (x_n, y_n, z_n)$. This probability density depends on the following dimensionless coordinate ratios:

$$\frac{x_2-x_1}{y_1}, \ldots, \frac{x_n-x_1}{y_1}, \frac{z_2-z_1}{y_1}, \ldots, \frac{z_n-z_1}{y_1}, \frac{y_2}{y_1}, \ldots, \frac{y_n}{y_1} \tag{29}$$

and also on the ratio y_1/δ_v (or y_1/δ_h, or y_1/H), characterizing the relative distance of the first point from the wall. Besides it also depends on the dimensionless combinations

$$Z = \delta/\delta_p = \gamma\delta/u_*^2, \quad Re_* = \delta/\delta_v = \delta u_*/\nu,$$
$$\delta/H, \quad Pr = \delta_v/\delta_h = \nu/a$$

that determine the flow conditions and the physical properties of the fluid.

The above relations between the characteristic length scales allow one to consider the analyzed turbulent boundary layer as a thermally and dynamically developed one and, consequently, to eliminate the parameter Re_* (and Pe_*) from the list of relevant parameters. Moreover, it follows from these relations that, there exist zones in the considered boundary layer, where the temperature profile is described by the logarithmic and inverse half-power laws. It is easy to understand that in the first of these zones (i.e. in the logarithmic sublayer) all the constant-pressure relations summarized in Appendix B must be valid. The analysis will therefore be confined to the characteristics of temperature fluctuations in the gradient zone and the outer part of the boundary layer, where the effect of the longitudinal pressure gradient is displayed.

In the sublayer where the inverse half-power law is valid, i.e. where $\delta_p \ll y \ll \min(\delta, H)$, the regime of temperature fluctuations is governed only by two-dimensional parameters: γ and Q. Now, it will be assumed that the considered set of points is localized in a small volume within this sublayer, so that $(|\mathbf{X}_i - \mathbf{X}_j|) \ll \min(\delta, H)$ and $\delta_p \ll y_1 \ll \min(\delta, H)$. Then the joint probability density, normalized by the appropriate combination of the parameters Q, γ, and one of the normal coordinates y_i, can depend only on ratios (29), $y_1 u_*/\nu$, and Pr but is independent of the type of flow, i.e. is the same for flows in tubes, channels, boundary layers on a plate, etc. Besides, if the selected points are not too close to each other (so that $|\mathbf{X}_i - \mathbf{X}_j| \gg \max(\delta_v, \delta_h)$ for any i and j), then the molecular constants of the fluid also do not affect the joint probability density, and therefore the list of the dimensionless parameters affecting this density includes only ratios (29).

The horizontal homogeneity of the considered two-dimensional flow and its symmetry with respect to the x–y plane lead to the following additional requirement: the probability density must be invariant with respect to the sign reversal of velocity components $w(\mathbf{X}_i)$, $i = 1, \ldots, n$. Moreover, this density must be a universal function of its arguments, i.e. it must be independent of both the flow type and fluid properties (but, of course, it can be different for accelerating and decelerating flows). For instance, in the case of the one-point density

$$(\gamma Q y) p(\theta, u, v, w) = P_\theta^{(p)}(\theta\sqrt{(\gamma y)}/Q, u/\sqrt{(\gamma y)}, v/\sqrt{(\gamma y)}, w/\sqrt{(\gamma y)})$$
$$\text{for} \quad u_*^2/\gamma \ll y \ll \min(\delta, H) \tag{30}$$

where $P_\theta^{(p)}$ is a universal function of four variables and u, v, w are three components of $\mathbf{u}$.

For the even more simple one-dimensional probability density $p(\theta)$ of temperature fluctuations at the point $\mathbf{X} = (x, y, z)$, which is located within the inverse power-law sublayer, the following relation can be easily obtained:

$$(Q/\sqrt{(\gamma y)}) p(\theta) = P_\theta^{(p)}(\theta\sqrt{(\gamma y)}/Q). \tag{31}$$

However, the data needed to verify this simple relation are also lacking until now.

(2) The dimensional analysis also permits one to write out relations for one-point moments of temperature fluctuations and mixed moments of temperature and velocity fluctuations. It appears that

$$\langle\theta^k u^m v^n w^l\rangle/Q^k u_*^{m+n+l-k} = \phi_{kmnl}^{(2,p)}(\xi)$$

$$\text{for} \quad \max(\delta_v, \delta_h) \ll y \ll \min(\delta, H) \quad (32a)$$

$$\langle\theta^k u^m v^n w^l\rangle/Q^k(\gamma H)^{(m+n+l-k)/2} = \phi_{kmnl}^{(3,p)}(\eta, \delta/H)$$

$$\text{for} \quad y \gg \delta_p \quad (32b)$$

while in the overlapping layer of these two asymptotic expansions (i.e. in the layer $\delta_p \ll y \ll \min(\delta, H)$, where the inverse half-power law is valid for the temperature profile) the following relations are true:

$$\langle\theta^k u^m v^n w^l\rangle = a_{kmnl}^{(p)} Q^k(\gamma y)^{(m+n+l-k)/2} \quad (32c)$$

where $a_{kmnl}^{(p)}$ is a universal constant. The exact limits of the validity layer for (9a), (9b) and for various relations (32c) may, of course, differ. The constants $a_{kmnl}^{(p)}$ must be independent of both the physical properties of the fluid and the type of pressure-gradient flow (but their values can depend on the sign of dP/dx). It is also clear that they are equal to zero for all the odd values of l. The value of these constants can be estimated from experimental data or from some semi-empirical closures of the dynamic and thermal equations. For the second-order moments of velocity fluctuations in the gradient-sublayer equations (32) were verified in ref. [13]. As for the temperature fluctuations it will be, apparently, more simple to verify theoretical predictions for the variance, asymmetry and flatness factor of temperature fluctuations in this sublayer

$$\langle\theta^2\rangle/t_*^2 = a_2^{(p)}/\xi \quad \text{for} \quad u_*^2/\gamma \ll y \ll \min(\delta, H),$$

$$S_3^{(p)} = \langle\theta^3\rangle/\langle\theta^2\rangle^{3/2} = a_3^{(p)}/a_2^{(p)3/2} = \text{const.},$$

$$F_4^{(p)} = \langle\theta^4\rangle/\langle\theta^2\rangle^2 = a_4^{(p)}/a_2^{(p)2} = \text{const.} \quad (33)$$

and also for the second-order mixed moments of temperature and velocity fluctuations

$$\langle u\theta\rangle/Q = a_{1100}^{(p)} = \text{const.}$$

$$\text{and} \quad \langle v\theta\rangle/Q = a_{1010}^{(p)} = \text{const.} \quad (34)$$

It is worth noting that the latter relations have the same form in the constant-pressure flows, but the values of the constants in formulae (33) and (34) can, of course, differ from those related to flows where $dP/dx = 0$ (see Appendix B).

Experimental data related to temperature fluctuation moments in the pressure-gradient flows are available only for the moment in the first line of equation (33). Measurements of σ_θ/t_*, where $\sigma_\theta = \langle\theta^2\rangle^{1/2}$, conducted in a strongly decelerated air boundary layer on a heated plate [7] are presented in Fig. 13 in the form of the dependence of $(\sqrt{(\gamma y/Q)})\sigma_\theta$ on ξ. They demonstrate that, in accordance with the theoretical predictions, $(\sqrt{\xi}/t_*)\sigma_\theta = \text{const.} \cong 1.25$. Hence $a_2^{(p)} \cong 1.6$, and Fig. 13 also shows that the region, where the profile of σ_θ/t_* obeys the inverse square root law, can be described by inequalities $(u_*^2/\gamma) < y < 0.4H$.

(3) A vertical profile of the temperature dissipation

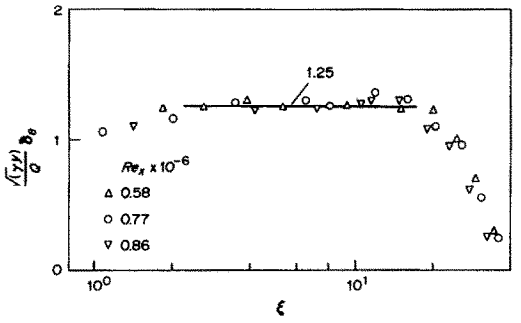

FIG. 13. The profile of the dimensionless r.m.s. for temperature fluctuations in the gradient sublayer according to the data of ref. [7].

$$N(y) = a\sum_i \langle(\partial\theta/\partial x_i)^2\rangle$$

in the gradient and outer zones of non-isothermal turbulent flows is determined by the relationships

$$N(y) = (Q^2\gamma/u_*^3)\phi_N^{(2,p)}(\xi)$$

$$\text{for} \quad \max(\delta_v, \delta_h) \ll y \ll \min(\delta, H) \quad (35a)$$

$$N(y) = (Q^2/\sqrt{(\gamma H^3)})\phi_N^{(3,p)}(\eta, \delta/H) \quad \text{for} \quad y \gg \delta_p. \quad (35b)$$

In the overlapping layer of these asymptotic expansions (if such a layer exists), the following equalities must be valid:

$$(\sqrt{(\gamma y^3)}/Q^2)N(y) = \xi^{3/2}\phi_N^{(2,p)}(\xi)$$

$$= \eta^{3/2}\phi_N^{(3,p)}(\eta, \delta/H) = \alpha_N^{(p)} = \text{const.}$$

so that

$$N(y) = \alpha_N^{(p)} Q^2/\sqrt{(\gamma y^3)}$$

$$\text{for} \quad u_*^2/\gamma \ll y \ll \min(\delta, H). \quad (35)$$

Similar arguments can also be applied to the derivation of the following formula for the turbulent energy dissipation:

$$\varepsilon(y) = \tfrac{1}{2}\nu\sum_{i,j}\left\langle\left(\frac{\partial u_i}{\partial x_j} + \frac{\partial u_j}{\partial x_i}\right)^2\right\rangle:$$

$$\varepsilon(y) = a_\varepsilon^{(p)}\gamma^{3/2}y^{1/2} \quad \text{when} \quad u_*^2/\gamma \ll y \ll \min(\delta, H). \quad (36)$$

The comparison of equation (36) with the data described in ref. [14] yielded the estimate $a_\varepsilon^{(p)} \cong 2.4$.

(4) Interesting inferences can also be made about the spatial spectra of temperature fluctuations and corresponding correlation functions. For example, the longitudinal spatial temperature spectrum $E_{\theta\theta}(k, y)$, which depends on the wave number k and coordinate y, is given for a pressure-gradient flow by the relations

$$E_{\theta\theta}(k, y) = (Q^2/\gamma)E_{\theta\theta}^{(2,p)}(ky, \xi)$$

$$\text{for} \quad \max(\delta_v, \delta_h) \ll y \ll \min(\delta, H) \quad (37a)$$

$$E_{\theta\theta}(k, y) = (Q^2/\gamma)E_{\theta\theta}^{(3,p)}(ky, \eta, \delta/H) \quad \text{for} \quad y \gg \delta_p. \quad (37b)$$

There, for $\delta_p \ll y \ll \min(\delta, H)$

$$E_{\theta\theta}(k, y) = (Q^2/\gamma)e_{\theta\theta}^{(p)}(ky). \quad (37)$$

Let us now consider the behaviour of the function $e_{\theta\theta}^{(p)}(ky)$ for the wave numbers k belonging to the inertial-convective range. The upper limit of this range corresponds to the length scale $\delta_K = (\nu^3/\varepsilon)^{1/4}$ and then the corresponding temperature microscale $\delta_\theta = (a^3/\varepsilon)^{1/4}$, which, in the considered layer, is of the form

$$\delta_K \sim (\nu/u_*)(S/\sqrt{\xi})^{1/4}$$

$$\text{and} \quad \delta_\theta = (a/u_*)((Pr\ S)/\sqrt{\xi})^{1/4}. \quad (38)$$

As to the lower limit of the range, it must correspond to the length scale which is much smaller than δ and H. For thermally and dynamically developed turbulence ($Re_* \gg 1$ and $Pe_* \gg 1$) the corresponding range of the values ky includes the values satisfying the inequalities $ky \ll 1$ and $ky \gg 1$. For the locally isotropic small-scale turbulence $k \gg y^{-1}$, and here the Obukhov–Corrsin $-5/3$ power law is valid. Hence $E_{\theta\theta}(k, y) \sim N\varepsilon^{-1/3}k^{-5/3}$ and, consequently, $e_{\theta\theta}^{(p)} \sim (ky)^{-5/3}$ for $ky \gg 1$. In the other limiting case where $ky \ll 1$, it can be assumed that $e_{\theta\theta}^{(p)}(ky)$ tends to the limit

$$G_\theta^{(p)} = e_{\theta\theta}^{(p)}(0) = \lim_{ky \to 0} e_{\theta\theta}^{(p)}(ky).$$

If this assumption is true, then for the sublayer, where the inequalities $u_*^2/\gamma \ll y \ll \min(\delta, H)$ are satisfied, the following limiting laws hold true

$$(\gamma/Q^2)E_{\theta\theta}(ky) = \begin{cases} C_{\theta\theta}^{(p)}(ky)^{-5/3} & \text{for } ky \gg 1 \\ G_{\theta\theta}^{(p)} & \text{for } ky \ll 1 \end{cases}. \quad (39)$$

Thus, unlike the logarithmic sublayer, where (see Appendix B) for long-wave perturbations the spectrum of temperature fluctuations satisfies the -1 power law (B8), in the gradient sublayer, where the inverse half-power law is valid, the spectrum $E_{\theta\theta}$ does not depend on the value of ky for $ky \ll 1$. Similar arguments can be applied to the derivation of formulae for the velocity fluctuation spectra $E_{ii}(k)$ (where $i = 1, 2, 3$, and $u_1 = u$, $u_2 = v$, $u_3 = w$) in the gradient sublayer

$$(y^2\gamma)^{-1}E_{ii}(ky) = \begin{cases} C_{ii}^{(p)}(ky)^{-5/3} & \text{for } ky \gg 1 \\ G_{ii}^{(p)}(ky)^{-2} & \text{for } ky \ll 1 \end{cases} \quad (40)$$

and also to the Reynolds stress cospectrum

$$(y^2\gamma)^{-1}E_{uv}(ky) = G_{12}^{(p)}(ky)^{-2} \quad \text{for} \quad ky \ll 1 \quad (41)$$

and the velocity and temperature cospectra

$$(Qy)^{-1}E_{i\theta}(ky) = G_{i\theta}^{(p)}(ky)^{-1} \quad \text{for} \quad ky \ll 1 \quad (42)$$

where $i = 1, 2$.

Equation (40) for $E_{uu}(ky)$ was derived and verified in ref. [14] where the approximate values of the universal constants $C_{11}^{(p)} = 0.9$ and $G_{11}^{(p)} = 1.6$ were also obtained.

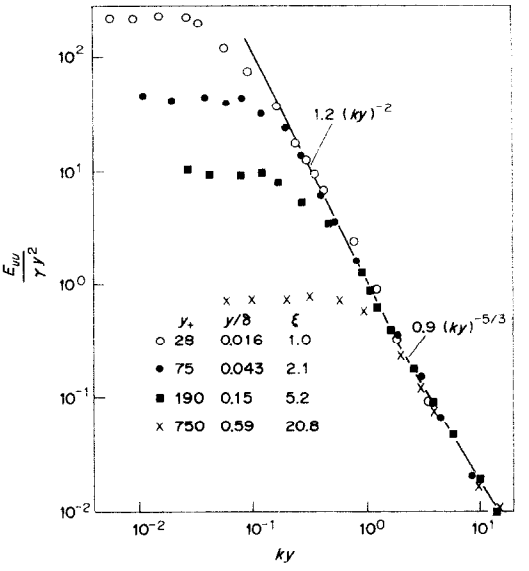

FIG. 14. The longitudinal spectrum of longitudinal velocity fluctuations [7] in the gradient sublayer ($\xi = 1, 2.1, 5.2$) and outside of it ($y/\delta = 0.59$).

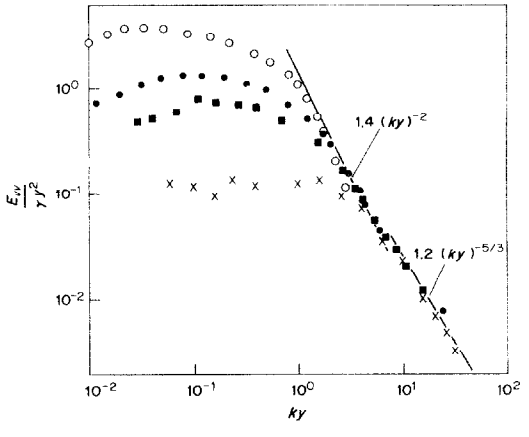

FIG. 15. The longitudinal spectrum of normal velocity fluctuations [7] in the gradient sublayer. For notation see Fig. 14.

Figures 14–18 give the measured values of the spectra and cospectra E_{uu}, E_{vv}, E_{ww}, $E_{\theta\theta}$, and $E_{v\theta}$ in an equilibrium decelerated boundary layer with heat transfer studied in ref. [7]. The parameters of the considered flow ($Z \cong 45$ and $S \cong 35$) show that in the cross-section measured ($x = 955$ mm) the flow state was close to separation. An appreciable difference between the thicknesses of the thermal ($H = 68$ mm) and dynamic ($\delta = 93.3$ mm) boundary layers in the flow cross-section studied does not affect noticeably, as was explained above, the characteristics of turbulence in the gradient sublayer.

The velocity fluctuation spectra measured in ref. [7] agree satisfactorily with theoretical equations (40) and (41). Here the coefficient $G_{11}^{(p)} \cong 1.2$ turns out to be

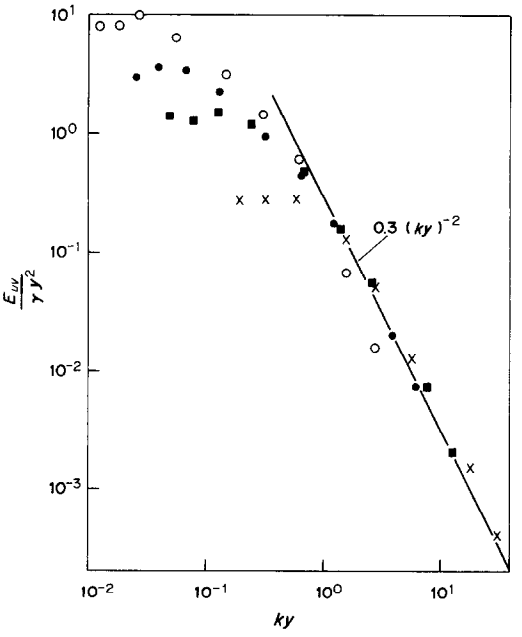

FIG. 16. The longitudinal spectrum of Reynolds stress [7] in the gradient sublayer. For notation see Fig. 14.

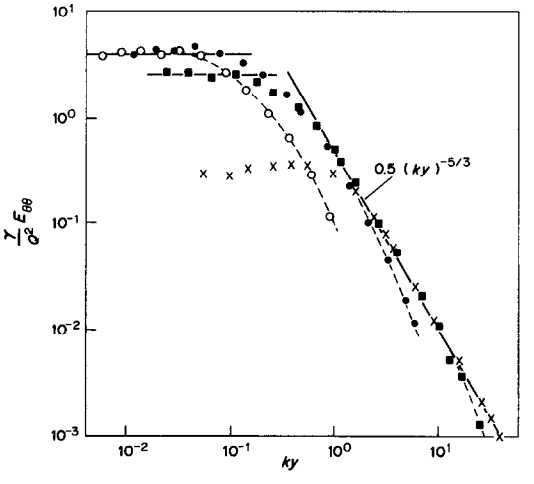

FIG. 17. The longitudinal spectrum of temperature fluctuations. For notation see Fig. 14.

slightly different from the estimate obtained previously, whereas the values $C_{11}^{(p)} \cong 0.9$ and $C_{22}^{(p)} \cong 1.2$ together with $a_\varepsilon^{(p)} = 2.4$ lead to the value of the universal Kolmogorov constant $C = E_{ii}/\varepsilon^{2/3}k^{-5/3} \cong 0.5$ which is presently assumed to be the most reliable. These experimental data also allow an evaluation of the universal constants $G_{22}^{(p)} \cong 1.4$ and $G_{12}^{(p)} \cong 0.3$. It must also be noted that the maximum extent of the range, where the '-2 power law' (second line in equation (40)) is valid, is observed at the proximity to the wall, where, as a rule, the '$-5/3$ power law' is almost unperceptible. However, the '$-5/3$ power law' is displayed quite distinctly on the outer boundary of the gradient sublayer (at $\xi = 5.2$) and outside of it (at $y/\delta = 0.6$).

The spectra $E_{\theta\theta}(ky)$ and the cospectrum $E_{v\theta}(ky)$ do

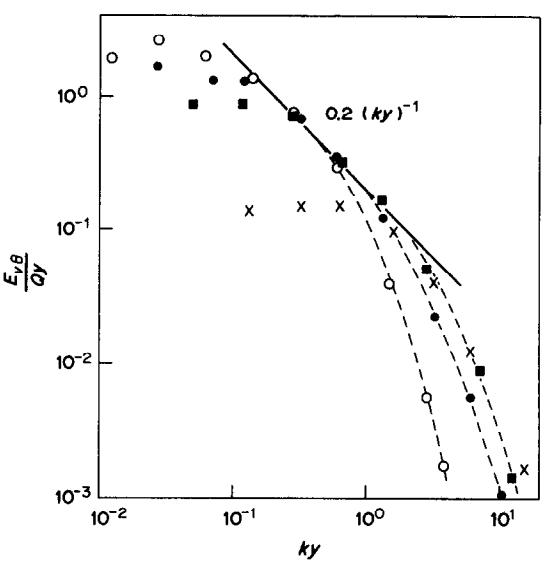

FIG. 18. The cospectrum of the temperature flux in the decelerated boundary layer. For notation see Fig. 14.

not contradict theoretical conclusions either, though the scatter of the data in Figs. 17 and 18 substantially exceeds the corresponding spread in the data on velocity fluctuations. Thus, the estimation of the constant $G_{\theta\theta}^{(p)}$ in equation (39) from the experimental results obtained at the points $y/\delta = 0.016$ and 0.043 yields $G_{\theta\theta}^{(p)} \cong 4$, whereas the data at $y/\delta = 0.15$ lead to the estimate $G_{\theta\theta}^{(p)} \cong 2.5$.

In the validity region of the $-5/3$ power law (for $ky \gtrsim 0.5$) one obtains $C_{\theta\theta}^{(p)} \cong 0.5$, i.e. for $\alpha_N = 1$ the following estimate of the universal Obukhov–Corrsin constant $C_T = E_{\theta\theta}/N\varepsilon^{-1/3}$ is obtained $C_T \cong 0.7$. This estimate agrees well with the data of the most reliable measurements (see ref. [42]).

The accuracy of the estimate $G_{2\theta}^{(p)} \cong 0.2$ (see Fig. 18) is apparently rather low, but at present there are no other experimental results permitting the estimation of one or other of the coefficients given above.

(5) For the second-order longitudinal correlation function

$$R_{\theta\theta}(r, y) = \langle \theta(x+r, y, z)\theta(x, y, z) \rangle$$

the following equations can be obtained:

$$R_{\theta\theta}(r, y) = (Q/u_*)^2 R_\theta^{(2,p)}(r/y, \xi)$$

$$\text{for} \quad \max(\delta_v, \delta_h) \ll r, y \ll \min(\delta, H) \qquad (43a)$$

$$R_{\theta\theta}(r, y) = (Q^2/\gamma H) R_\theta^{(3,p)}(r/y, \eta, \delta/H)$$

$$\text{for} \quad r, y \gg \delta_p \qquad (43b)$$

and

$$R_{\theta\theta}(r, y) = (Q^2/\gamma y) R_\theta^{(p)}(r/y)$$

$$\text{for} \quad \delta_p \ll r, y \ll \min(\delta, H). \qquad (43)$$

The range of variations in the argument of the latter function is given by the inequalities

$$\max\left[(y_+\sqrt{\xi})^{-3/4},(y_+\sqrt{\xi\,Pr})^{-3/4}\right] \ll r/y \ll \min(\delta/y, H/y)$$

and for a dynamically and thermally developed turbulence it includes the values satisfying the inequalities $r/y \gg 1$ and $r/y \ll 1$. For small values of r/y within this range the Obukhov '2/3 power law' [15] is valid and hence

$$R_\theta^{(p)}(r/y) = \langle\theta^2\rangle(\gamma y/Q^2) - r_\theta^{(p)}(r/y)^{2/3} \qquad (44)$$

where $r_\theta^{(p)}$ is the universal constant simply related to $C_{\theta\theta}^{(p)}$.

For $r/y \gg 1$, the assumption about the existence of

$$\lim_{r/y\to\infty} R_\theta^{(p)}(r/y) = a_\theta^{(p)} = \text{constant}$$

leads to the conclusion that here

$$\langle\theta(x+r)\theta(x)\rangle/t_*^2 = a_\theta^{(p)}/\sqrt{\xi} \qquad (45)$$

(cf. equation (B11) valid in the logarithmic sublayer for $r/y \gg 1$).

REFERENCES

1. A. E. Perry, J. B. Bell and P. N. Joubert, Velocity and temperature profiles in adverse pressure-gradient turbulent boundary layers, *J. Fluid Mech.* **25,** 299–320 (1966).
2. N. Afzal, Thermal turbulent boundary layer under strong adverse pressure-gradient near separation, *Trans. ASME, J. Heat Transfer* **104,** 397–402 (1982).
3. B. A. Kader and A. M. Yaglom, Similarity treatment of dynamic-equilibrium turbulent boundary layers in adverse pressure-gradients, *J. Fluid Mech.* **89,** 305–342 (1978).
4. B. A. Kader and A. M. Yaglom, Heat and mass transfer laws for fully turbulent wall flows, *Int. J. Heat Mass Transfer* **15,** 2329–2351 (1972).
5. B. A. Kader, Temperature and concentration profiles in fully turbulent boundary layers, *Int. J. Heat Mass Transfer* **24,** 1541–1544 (1981).
6. N. H. Wooley, Heat transfer in turbulent boundary layers with arbitrary pressure gradients, confined flows and viscous recirculating flows, Ph.D. Thesis, Victoria University, Manchester (1973).
7. P. S. Roganov, Experimental study of heat transfer in a decelerating boundary layer, Author's Abstract of Candidate Dissertation, Moscow (1979).
8. D. E. Coles, The law of the wake in turbulent boundary layer, *J. Fluid Mech.* **1,** 191–226 (1956).
9. P. S. Granville, A modified law of the wake for turbulent shear layers, *Trans. ASME, J. Fluid Engng* **198,** 578–580 (1976).
10. C. S. Subramania and R. A. Antonia, Effect of Reynolds number on a slightly heated turbulent boundary layer, *Int. J. Heat Mass Transfer* **24,** 1833–1846 (1981).
11. E. U. Repik and V. K. Kuzenkov, Experimental investigation of the relation between heat transfer and friction in a turbulent boundary layer with the longitudinal pressure gradient, *Teplofiz. Vysok. Temp.* **18,** 1196–1202 (1980).
12. V. K. Migai, Reynolds analogy in a boundary layer with pressure gradient. In *Heat and Mass Transfer—V*, Vol. 1, pt. 1, pp. 148–151. Izd. ITMO, Minsk (1976).
13. B. A. Kader, Turbulence in the gradient sublayer of two-dimensional decelerating boundary layers, *Dokl. Akad. Nauk SSSR* **249**(2), 298–302 (1979).
14. B. A. Kader, Structure of anisotropic velocity and temperature fluctuations in a fully developed boundary layer, *Izv. Akad. Nauk SSSR, Mekh. Zhidk. Gaza* No. 1, 47–56 (1984). Spectra of anisotropic turbulent velocity and temperature fluctuations in the gradient sublayer of decelerating turbulent boundary layers, *Dokl. Akad. Nauk SSSR* **279**(2), 323–327 (1984).
15. A. M. Obukhov, Structure of the temperature field in a turbulent flow, *Izv. Akad. Nauk SSSR, Geogr. Geofiz.* **13,** 58–69 (1949).
16. B. A. Kader, Turbulent heat and mass transfer with $Pr \gg 1$ and turbulent viscosity damping near a solid wall, *Izv. Akad. Nauk SSSR, Mekh. Zhidk. Gaza* No. 2, 172–175 (1977).
17. L. D. Landau and E. M. Lifshits, *Fluid Mechanics*. Pergamon Press, London (1963).
18. L. Fulachier, Contribution a l'étude des analogies de champs dynamique et thermique dans une couche limite turbulente, Effet de l'aspiration, Thèse Doct. Sci., Univ. Provence, Marseille (1972).
19. A. Žukauskas and A. Šlančiauskas, *Heat Transfer in a Turbulent Fluid Flow*. Izd. Mintis, Vilnius (1973).
20. B. A. Kader and A. M. Yaglom, Similarity laws for turbulent flows. In *Itogi Nauki i Tekhniki, Mekh. Zhidk. Gaza (Izv. VINITI)*, Vol. 15, pp. 81–155 (1980).
21. S. Tanimoto and T. J. Hanratty, Fluid temperature fluctuations accompanying turbulent heat transfer in a pipe, *Chem. Engng Sci.* **18,** 307–311 (1963).
22. G. S. Taranov, The study of statistical properties of the velocity and temperature fields in a turbulent shear flow, Author's Abstract of Candidate Dissertation, Moscow (1970).
23. K. Bremhorst and K. J. Bullock, Spectral measurements of turbulent heat and momentum transfer in fully developed pipe flows, *Int. J. Heat Mass Transfer* **16,** 2141–2154 (1973).
24. Z. Zarič, Contribution a l'étude statistique de la turbulence partietale, Thèse Doct. Sci. Phys., Univ. Paris (1974).
25. V. M. Belov, Experimental study of heat transfer in a turbulent boundary layer with a step change in thermal boundary conditions, *Teor. Osnovy Khim. Tekhnol.* **19,** 393–401 (1976).
26. A. E. Perry and P. H. Hoffman, An experimental study of turbulent convective heat transfer from a flat plate, *J. Fluid Mech.* **77,** 355–368 (1976).
27. M. Elena, Etude experimentale de la turbulence au voisinage de la paroi d'une tube légèrement chauffé, *Int. J. Heat Mass Transfer* **20,** 935–944 (1977).
28. A. F. Polyakov and Yu. V. Tsypulev, Experimental study of averaged values and variances of velocity and temperature in turbulent air plane channel flows, *Trudy Mosk. Energ. Inst.* No. 377, 109–116 (1978).
29. B. S. Petukhov, A. F. Polyakov, Yu. L. Shehter and Yu. V. Tsypulev, Experimental investigation of statistical properties of air temperature fluctuations in a viscous sublayer, *Trudy Mosk. Energ. Inst.* No. 235, 3–13 (1975).
30. M. Hishida and Y. Nagano, Structure of turbulent temperature and velocity fluctuations in the thermal entrance region of a pipe, *Proc. 6th Int. Heat Transfer Conf.*, Toronto, Vol. 2, pp. 531–536 (1978).
31. V. B. Bobkov, M. Kh. Ibragimov and V. I. Subbotin, Statistical properties of temperature fluctuations in a turbulent flow. In *Liquid Metals*, pp. 53–71. Gosatomizdat, Moscow (1967).
32. J.-G. Richard, Etude des profiles de temperatures dans un ecoulement turbulent etabli dans un tube cylindrique lisse, *Bull. Dir. Etud. Rech. Ser. A* No. 2, 1–73 (1972).
33. V. P. Bobkov, S. P. Beschastnov, Yu. I. Gribanov, M. Kh. Ibragimov and P. K. Karpov, Statistical investigation of the temperature field in a turbulent pipe water flow, *Teplofiz. Vysok. Temp.* **8,** 806–812 (1970).
34. B. V. Perepelitsa, The study of hydrodynamics and heat

transfer in a turbulent water flow containing high polymers, *Teor. Osnovy Khim. Tekhnol.* **10**, 147–159 (1971).
35. S. S. Kutateladze, E. M. Khabakhpasheva and B. V. Perepelittsa, Temperature fluctuations in a viscous sublayer, *Proc. 6th Int. Heat Transfer Conf.*, Toronto, Vol. 2, pp. 531–536 (1978).
36. A. M. Yaglom, Similarity laws for constant pressure and pressure-gradient turbulent wall flows, *Ann. Rev. Fluid Mech.* **11**, 505–540 (1979).
37. A. E. Perry and C. J. Abell, Scaling laws for pipe-flow turbulence, *J. Fluid Mech.* **67**, 257–271 (1975).
38. B. N. Korotkov, Some forms of local self-similarity of the velocity fields of turbulent wall flows, *Izv. Akad. Nauk SSSR, Mekh. Zhidk. Gaza* No. 6, 35–42 (1976).
39. A. B. Žaliauskas, Momentum and heat transfer in turbulent accelerating boundary layers, Author's Abstract of Candidate Dissertation, Institute of Physical and Technical Problems of Energetics, Acad. Sci. Lithuan. SSR, Kaunas (1980).
40. A. A. Pedišius, Turbulent Prandtl number and universal temperature profiles at various Prandtl numbers, Author's Abstract of Candidate Dissertation, Institute of Physical and Technical Problems of Energetics, Acad. Sci. Lithuan. SSR, Kaunas (1969).
41. M.-R. M. Drižus, Experimental investigation of heat transfer in the wall region of turbulent boundary layer, Author's Abstract of Candidate Dissertation, Kaunas (1971).
42. A. M. Yaglom, Laws of small-scale turbulence in atmosphere and ocean, *Izv. Akad. Nauk SSSR, Ser. Atmos. Oceanic Phys.* **17**, 1235–1257 (pp. 919–935 of the English edition) (1981).
43. B. A. Kader, A. M. Yaglom and S. L. Zubkovskiy, Spatial correlation function of surface-layer atmospheric turbulence in neutral stratification, *Boundary-layer Meteorol.* **47**, 233–249 (1989).

APPENDIX A. THE THICKNESS OF A TURBULENT THERMAL BOUNDARY LAYER

The thickness of a dynamic boundary layer is usually defined as the distance from the wall to the point where the mean flow velocity $U(\delta)$ is equal to some fixed part of U_o (e.g. one of the most common definitions of δ is based on the relation $U(\delta) = 0.99U_o$). However, the thickness H of a thermal boundary layer, even when heat can be considered to be a passive admixture, depends not only on dynamic characteristics of a boundary layer, but also on fluid properties (first of all, molecular Prandtl number). This dependence is especially significant for $Pr \gg 1$, when the main heat transfer resistance is concentrated in a very narrow wall region. If, by the analogy with the definition of δ, H is defined with the aid of the relation $T_w - T(H) = 0.99(T_w - T_o)$, then at $Pr \gg 1$, the thickness H will be much smaller than δ. However, it is natural to think that the thicknesses δ and H must have the same order of magnitude since both of them determine the value of y where the turbulent mixing becomes negligible. Therefore, it seems natural to exclude from the consideration the sublayer of molecular heat transfer in the definition of the thickness H.

An empirical interpolation formula for the function $\beta(Pr)$ on the right-hand side of equation (8a) is given in ref. [4]. This formula is based on the analysis of a number of measurements of temperature profiles in boundary layers; it has a correct asymptotic behaviour at $Pr \gg 1$ and $Pr \ll 1$ and can be written in the form

$$\beta(Pr) = (3.85Pr^{1/3} - 1.3)^2 + 2.12 \ln Pr \qquad \text{(A1)}$$

(here some small modifications of the original equation inspired by the most recent data are taken into account). Equation (A1) may be used for the following estimate of the temperature difference between the wall and the upper edge of the molecular heat transfer sublayer (of thickness Δ):

$$[T_w - T(\Delta)]/t_* = \beta(Pr), \quad t_* = Q/u_*. \qquad \text{(A2)}$$

The thickness Δ can be defined, for the example, as the distance from the wall to the point where the eddy thermal diffusivity ε_H becomes equal to the molecular thermal diffusivity. The results of the statistical analysis of the experimental data on mass transfer at $Pr \gg 1$ described in ref. [16] show that near the wall $\varepsilon_H/\nu \cong 6 \times 10^{-4}(yu_*/\nu)^3$. Hence $\Delta \cong 12Pr^{-1/3}(\nu/u_*)$ for $Pr \gg 1$. According to this definition of Δ, it is easy to show that the same estimate of Δ proves to be valid also in the case of heat transfer in gases (i.e. for $Pr \sim 1$), where Δ has the order of $10(\nu/u_*)$. Assuming that the temperature profile is given by the linear equation $T_+ = Pr\, y_+$ for $y \leqslant \Delta$ results in $T_+(\Delta) = [T_w - T(\Delta)]/t_* \cong 12Pr^{2/3}$ when $Pr \gtrsim 1$; this estimate agrees satisfactorily with equations (A1) and (A2).

The exclusion of the wall sublayer of thickness Δ from consideration makes it reasonable to base the definition of H on the relation $T(\Delta) - T(H) = 0.99[T(\Delta) - T_o]$. According to equation (A2) this relation leads to the equation

$$T_+(H) = 0.99T_{o+} + 0.01\beta(Pr) \qquad \text{(A3)}$$

which gives the estimate of H the independence of which of Pr is very weak.

For the logarithmic velocity profile the dimensionless velocity at the top of the viscous sublayer is just a constant (independent of Pr) of the order of ten. Therefore, the exclusion of the viscous sublayer does not considerably affect the estimation of the thickness of the dynamic boundary layer. In fact, the relation $U_+(\delta) = U(\delta)/u_*$, which is analogous to equation (A3), has the form

$$U_+(\delta) = 0.99U_{o+} + 0.1. \qquad \text{(A4)}$$

In the developed turbulent boundary layer $U_{o+} = (c_f/2)^{-1/2}$ is very large, and hence equation (A4) practically does not differ here from the usually used equation $U_+(\delta) = 0.99U_{o+}$. However, in the case of the thermal boundary layer, where the molecular Prandtl number plays an important role, the situation is quite different.

An experimental determination of H, is often rather difficult (especially when Pr is large); therefore it is desirable to replace H by some more convenient length. The simplest (and most easily measured) length scale is the distance x of the given cross-section from the front edge of the plate (or from the point of the boundary layer turbulization). The equation expressing δ in terms of x was given in ref. [17] for the constant-pressure turbulent boundary layer; it is justified by the dimensional analysis and has the form

$$d\delta/dx = a(u_*/U_o) \qquad \text{(A5)}$$

where the constant a was found to be close to 0.3 [3, 20]. If the dependence of H on Pr is neglected, the arguments which lead to equation (A5) can also be applied to the derivation of the similar equation determining the dependence of the thickness H of a thermal boundary layer on x. This equation has the form

$$dH/dx = (u_*/U_o) \qquad \text{(A6)}$$

where the coefficient b can differ from a, but hardly by much.

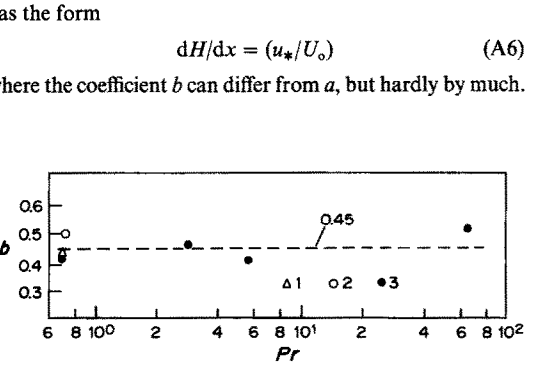

FIG. A1. Determination of the coefficients b in equation (A6) from the experimental data of: 1, ref. [18]; 2, ref. [6]; 3, ref. [19].

Note that according to equations (A5) and (A6) the thickness δ and H are proportional to each other if the dynamical and thermal turbulent layers begin to develop at the same point (e.g. at the front edge of the plate).

The experimental data from refs. [6, 18, 19] related to the development of thermal boundary layers in constant-pressure flows of different fluids (with $0.7 \leqslant Pr \leqslant 64$) are given in Fig. A1. The data given in this figure agree well with the conclusion about the proportionality of H to δ and show that $b = 0.45$ and hence $H/\delta = b/a \cong 0.45/0.33 \cong 1.3$.

APPENDIX B. CHARACTERISTICS OF TEMPERATURE FLUCTUATIONS WITHIN THE LOGARITHMIC SUBLAYER OF A CONSTANT-PRESSURE BOUNDARY LAYER

It has already been explained in this paper that the relations for the temperature fluctuations valid within the logarithmic sublayer of a constant-pressure boundary layer are valid also within the pressure-gradient boundary layers if $\max(\delta_v, \delta_h) \ll y \ll \delta_p$. Therefore, such relations are quite interesting for the problem studied in this paper and it is reasonable to consider them here in short (see also refs. [20, 36]).

The corollaries from the dimensional analysis given at the beginning of Section 2 of the present paper can, of course, be directly applied to the logarithmic sublayer where they have especially simple form. In particular, if $\min(\delta, H) \gg y \gg \max(\delta_v, \delta_h)$ then the probability density $p(\theta)$ of temperature fluctuations θ at the point x, y, z must have the form

$$t_* p(\theta) = P_\theta(\theta/t_*) \tag{B1}$$

where P_θ is a universal function of one variable. For one-point moments of temperature fluctuations $\langle\theta^k\rangle$ and mixed moments of temperature and velocity fluctuations $\langle\theta^k u^m v^n w^l\rangle$ in the logarithmic sublayer the following simplified form of equations (32c) and (33) must be valid:

$$\langle\theta^k\rangle/t_*^k = a_k = \text{const.} \tag{B2}$$

$$\langle\theta^k u^m v^n w^l\rangle/t_*^k u^{m+n+l} = a_{klmnl} = \text{const.} \tag{B3}$$

Here a_k and a_{klmnl} are universal constants independent either of the flow type or of the physical properties of the fluid.

However, in the thicker wall region $y \ll \min(\delta, H)$ (which includes the molecular conductivity sublayer) the values of the one-point moments are not universal constants but can depend on the distance from the wall and physical properties of the fluid. For example, in this region $\langle\theta^2\rangle^{1/2}/t_* = f(y_+, Pr)$, where f is a universal (i.e. independent of the flow type) function of two arguments Pr and $y_+ = y/\delta_v$.

Some experimental data related to the second moment of temperature fluctuations and to the coefficient of correlation $R_{u\theta} = \langle u\theta\rangle/(\langle u^2\rangle\langle\theta^2\rangle)^{1/2}$ between the temperature and longitudinal velocity fluctuations in the air flow ($Pr = 0.7$) along a smooth wall are shown in Fig. B1. The experimental points in Fig. B1 are rather scattered but on the whole the results of the measurements of $\langle\theta^2\rangle^{1/2}/t_*$ in tubes, channels, and boundary layers on a flat plate clearly cluster round a single curve which, for $y_+ > 100$, coincides with the horizontal straight line $\langle\theta^2\rangle^{1/2}/t_* \cong 1.3$. Thus, Fig. B1 shows that $a_2 \cong (1.3)^2 \cong 1.7$ and also permits one to suggest an empiric equation for $f_+(y_+, 0.7)$ indicated in this figure.

For the verification of the universality of the constant a_2, the data on the distribution $\langle\theta^2\rangle^{1/2}/t_*$ within the logarithmic sublayers of flows of fluid with physical properties different from those of air can be used. Such data are available for flows of mercury ($Pr = 0.026$), water ($Pr = 5$–10), ethyleneglycol ($Pr = 10$–30) and lubricating oil ($Pr = 50$–100). Some of these data (including the data for air flows too) are given in Fig. B2 where the uniform distribution of coordinates along the axis is used (such a distribution in contrast to the logarithmic distribution used in Fig. B1 does not conceal the scatter of experimental points). In spite of considerable scatter of the points (partially averaged in Fig. B2) they do not contradict the assumption that the value $\langle\theta^2\rangle^{1/2}/t_*$ in the logarithmic sublayer depends neither on Pr (within the range covering more than three orders of magnitude) nor on the type of the flow and is close to 1.3.

The measurements of mixed moments of temperature and velocity fluctuations can be found just in a few papers and they correspond mainly to the second-order moments (i.e. to the cases where $k+m+n+l = 2$). Clearly $a_{1010} = -1$ and $a_{1001} = 0$, but for the determination of the universal constant a_{1100} in equation (B3) the experimental data are needed. Such data are given in Fig. B1 for the case where $Pr = 0.7$. The data agree with the assumption on the independence of $R_{u\theta}$ of y_+ within the logarithmic sublayer and show that here $R_{u\theta} \cong -0.7$, i.e. $a_{1100} \cong R_{u\theta}(\langle\theta^2\rangle\langle u^2\rangle)^{1/2}/u_* t_* \cong -0.7 \times 1.3 \times 2.2 \cong -2.0$. Note that this estimate of a_{1100} is considerably lower than the atmospheric estimates of the same constant (see ref. [20]). Thus, in ref. [20] the estimate $a_{1100} = -3.5$ is given as the best fit to the atmospheric data. It is worth noting, however, that the atmospheric estimates of the constants $\langle u^2\rangle/u_*^2$ and, especially, $\langle\theta^2\rangle/t_*^2$ exceed considerably the laboratory estimate of these constants; therefore the value of the correlation coefficient $R_{u\theta}$ deduced from the atmospheric measurements proves to be quite close to the value given by the laboratory measurements.

The value of the correlation coefficient $R_{v\theta}$ in the logarithmic sublayer can be easily calculated from the known experimental data: $R_{v\theta} = \langle v\theta\rangle/(\langle v^2\rangle\langle\theta^2\rangle)^{1/2} \cong -(1 \times 1.3)^{-1} \cong -0.7$; it can be seen that it is close to the value of $R_{u\theta}$. However, the direct experimental measurements of $R_{v\theta}$ in the logarithmic sublayer are quite scattered. Thus, it was found in ref. [22] that in a tube flow $R_{v\theta} \cong -0.8$ for $Re = 32.5 \times 10^3$ and $R_{v\theta} \cong -0.65$ for $Re = 260 \times 10^3$, while for an air boundary layer on a plate, it was found in refs. [18, 25] that $Re_{v\theta} \cong -0.6$. Moreover, the tube flow measurements described in ref. [23] resulted in the estimate $R_{v\theta} \cong -0.4$. Therefore, the additional careful measurements of $R_{v\theta}$ are necessary. The asymmetry $S_\theta = \langle\theta^3\rangle/\langle\theta^2\rangle^{3/2}$ and flatness factor $F_\theta = \langle\theta^4\rangle/\langle\theta^2\rangle^2$ of the temperature fluctuations are the most interesting higher-order moments of θ. In the logarithmic sublayer

$$S_\theta = a_3/a_2^{3/2} = \text{const.}, \quad F_\theta = a_4/a_2^2 = \text{const.} \tag{B4}$$

Some experimental data on these characteristics are shown in Fig. B3. Most of these data refer to air flows in tubes, channels and boundary layers; they give rise to an impression that within the logarithmic sublayer S_θ differs from zero only slightly and $2.2 \leqslant F_\theta \leqslant 2.8$ (as the first approximation one can use the estimate $F_\theta = 2.5$). To verify these conclusions, the averaged results of measurements of S_θ and F_θ in the logarithmic sublayer of flows of some other fluids (namely, water, lubricating oil, and mercury) are also shown in Fig. B3. These data agree with the above-mentioned estimates $a_3/a^{3/2} \cong 0$ (i.e. $a_3 \cong 0$) and $a_4/a_2^2 \cong 2.5$ (i.e. $a_4 \cong 4.2$). Note, however, that the data shown in Fig. B3 are quite scattered (apparently because of insufficient accuracy of the measurements of the third- and fourth-order moments); therefore the estimates given above must be considered as only preliminary ones.

The similar dimensional arguments can be applied to the vertical profile of the so-called 'temperature dissipation', i.e. rate of molecular dissipation of $\langle\theta^2\rangle/2$

$$N = a\left\langle \sum_i (\partial\theta/\partial x_i)^2 \right\rangle.$$

According to ref. [36], within the logarithmic sublayer

$$N(y) = \alpha(u_* t_*^2/y) \tag{B5}$$

where α is the same coefficient which enters into the log-

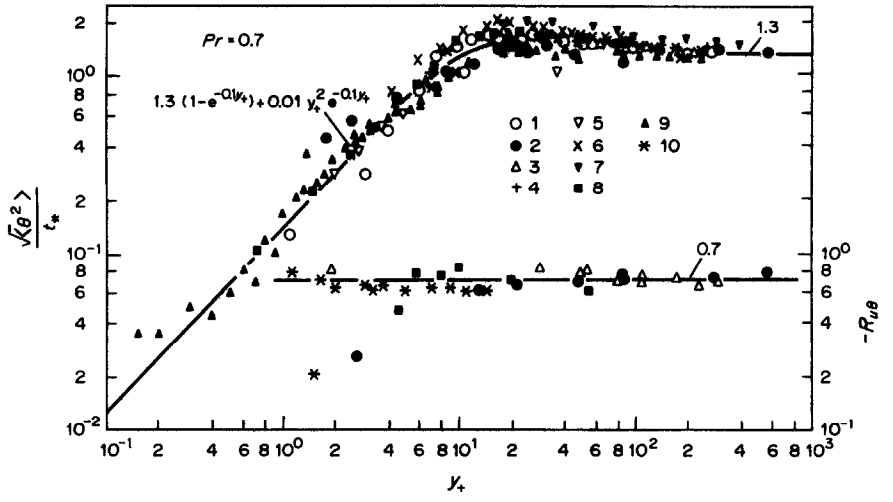

FIG. B1. The profiles of $\langle\theta^2\rangle^{1/2}/t_*$ and $R_{u\theta}$ in the wall zone of the air turbulent boundary layer based on the data of: 1, ref. [21]; 2, ref. [22]; 3, ref. [18]; 4, ref. [23]; 5, ref. [24]; 6, ref. [25]; 7, ref. [26]; 8, ref. [27]; 9, refs. [28, 29]; 10, ref. [30].

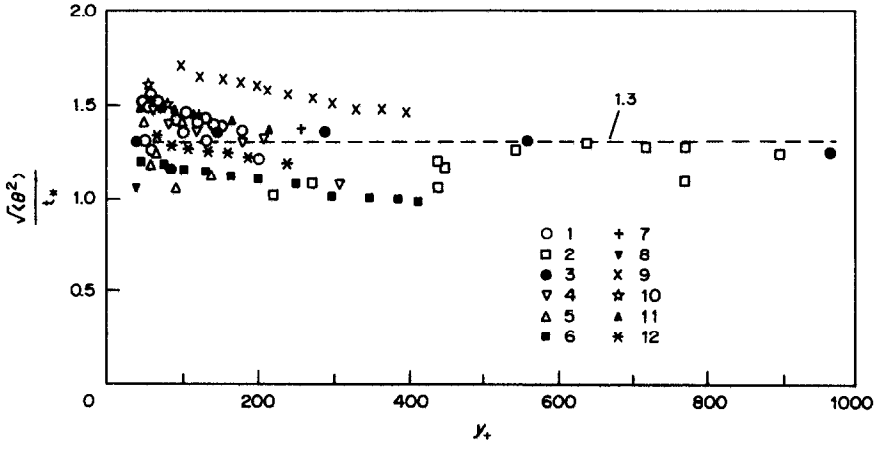

FIG. B2. The profile of $\langle\theta^2\rangle^{1/2}/t_*$ in the logarithmic sublayer according to the data of: 1, ref. [21] (air flow in a pipe); 2, ref. [31] (mercury and lead in a pipe); 3, ref. [22] (air in a pipe); 4, ref. [18] (air above a plate); 5, ref. [19] (air and oil above a plate); 6, ref. [32] (water in a pipe); 7, ref. [23] (air in a pipe); 8, ref. [24] (air in a plane channel); 9, ref. [26] (air above a plate); 10, ref. [27]; 11, ref. [30] (air in a pipe); 12, refs. [28, 29] (air in a pipe and a plane channel).

arithmic law (8) of the mean temperature distribution, i.e. $\alpha \cong 2.12$.

Finally, consider the longitudinal spatial spectrum of temperature fluctuations $E_{\theta\theta}(k, y)$ measured by a number of experimentalists.

For the range of wave numbers k satisfying the inequalities $\min(\delta, H) \gg k^{-1} \gg \max(\delta_v, \delta_h)$, the spectrum $E_{\theta\theta}(k, y)$ in the logarithmic sublayer has the form

$$E_{\theta\theta}(k, y) = t_*^2 k^{-1} e_{\theta\theta}(ky) \qquad \text{(B6)}$$

where $e_{\theta\theta}(ky)$ is a universal function. Assuming that the contribution to $\langle\theta^2\rangle$ of the long- and short-wave components of the temperature field with wave numbers beyond this range can be neglected, we obtain from (B6) the relation

$$\langle\theta^2\rangle = \int_0^\infty E_{\theta\theta}(k, y)\, dk$$

$$= t_*^2 \int_0^\infty (ky)^{-1} e_{\theta\theta}(ky)\, d(ky) = a_2 t_*^2.$$

Hence $\langle\theta^2\rangle/t_*^2 = a_2$ is a universal constant; this conclusion has been already formulated above and it agrees with the experimental data shown in Figs. B1 and B2.

In the case of a fully developed thermal boundary layer the range of wave numbers where equation (B6) is valid includes the values of k satisfying both the inequalities $ky \gg 1$ and $ky \ll 1$. If the first of these inequalities is valid, then according to Obukhov [15] and Corrsin (see ref. [42]) the function $e_{\theta\theta}(ky)$ and the spectrum $E_{\theta\theta}(ky)$ must have the form

$$E_{\theta\theta}(ky) = C_\theta t_*^2 y^{-2/3} k^{-5/3}$$

$$\text{and} \quad e_{\theta\theta}(ky) = C_\theta (ky)^{-2/3}. \qquad \text{(B7)}$$

It is seen that $E_{\theta\theta}(k, y)$ is proportional to $y^{-2/3}$ for $ky \gg 1$.

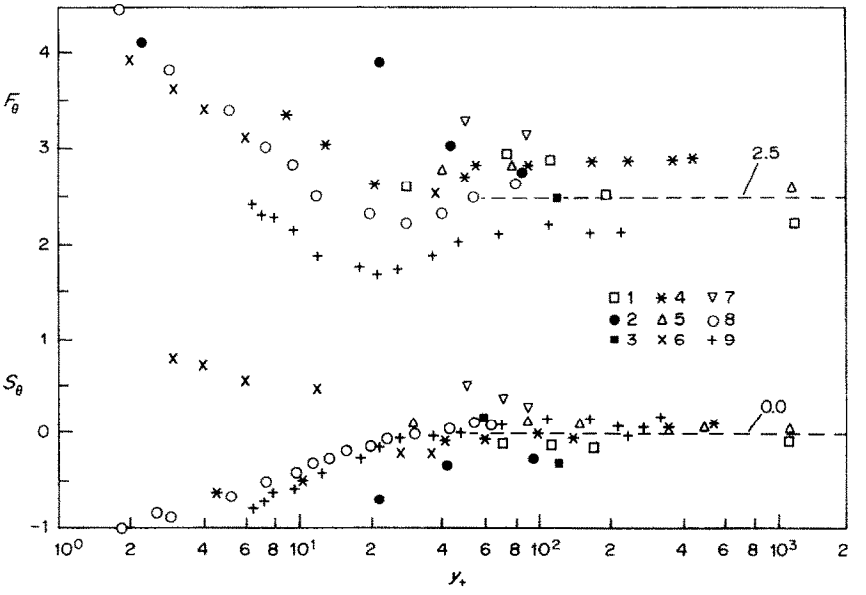

FIG. B3. The asymmetry and flatness factor of temperature fluctuations in the wall zone of the boundary layer. Notation is given in Fig. B2. The following data are added: 3, ref. [33] (a water flow in a pipe); 7, refs. [34, 35] (a water flow in a plane channel).

In the case where $ky \ll 1$, but $k \gg \min(\delta^{-1}, H^{-1})$ the wavelength of the considered spectral components is much greater than the distance y from the wall. It seems natural to assume that the statistical regime of such large-scale components of the temperature field does not change at moderate vertical shifts and therefore the spectrum $E_{\theta\theta}(k)$ does not depend on y for $ky \ll 1$. This assumption was formulated in refs. [37, 38] in application to longitudinal velocity spectra (and without the indication of the wave number range where it is valid); it is equivalent to the assumption on the existence of a finite non-zero limit

$$\lim_{ky \to 0} e_{\theta\theta}(ky) = e_{\theta\theta}(0) = G_\theta = \text{const.}$$

Then

$$E_{\theta\theta}(k, y) = G_\theta t_*^2 k^{-1} \quad \text{for} \quad k \ll y^{-1} \tag{B8}$$

where G_θ is a universal constant.

The existence of the wave number range where the temperature spectrum satisfies equation (B8) was discovered by some experimentalists (see, e.g. ref. [23]) who did not try to justify the law and indicate the limits of the range of its validity. Note, however, that the data confirming the law (B8) are much less extensive than those related to the similar law for the velocity spectrum and almost all these data are based on the measurements in air flows ($Pr \cong 0.7$). Experimental values of $E_{\theta\theta}(k, y)/yt_*^2$ taken from refs. [18, 23, 24] are shown in Fig. B4. It is seen that the data confirm the validity of the -1 power law (B8) and of the $-5/3$ power law (B7) for two ranges of wave numbers k and also show that both the ranges are rather wide and the transition zone between them is so narrow that in a first approximation these two ranges can be considered to adjoin to each other. According to Fig. B4 the -1 power law (B8) is valid for $ky \lesssim 5.2$ while the $-5/3$ power law (B7) is valid for $ky \gtrsim 5.2$; moreover

$$G_\theta \cong 0.3, \quad C_\theta \cong 0.9.$$

(These indicated estimates of the coefficients G_θ and C_θ and the boundary between two ranges are preliminary ones and they must be confirmed by careful measurements.) The estimate of C_θ permits one to estimate also the Obukhov–Corrsin constant C_T of the equation $E_{\theta\theta}(k) = C_T N \varepsilon^{-1/3} k^{-5/3}$

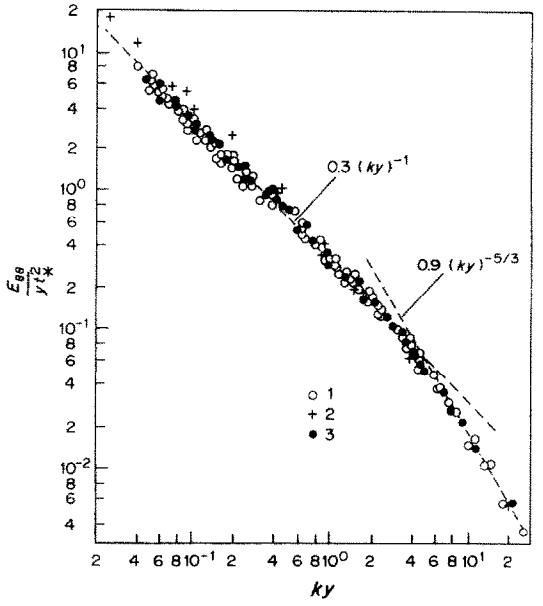

FIG. B4. The longitudinal spectrum of temperature fluctuations in the logarithmic sublayer for wave numbers in the inertial-convective interval according to the data of: 1, ref. [18]; 2, ref. [23]; 3, ref. [24].

describing the $-5/3$ power law for the temperature spectrum. Since $\varepsilon = Au_*^3/y$ and $N = \alpha u_* t_*^2/y$ in the logarithmic sublayer where $A \cong 2.5$ and $\alpha \cong 2.12$, $C_T = C_\theta A^{1/3}/\alpha \cong 0.6$, if $C_\theta \cong 0.9$. This estimate of C_T agrees satisfactorily with most of the other estimates of the Obukhov–Corrsin constant collected in ref. [42].

The data on $E_{\theta\theta}(k)$ permit one also to calculate the spatial longitudinal correlation function of temperature fluctuations. The $-5/3$ power law (B7) implies that

$$R_{\theta\theta}(r) = \langle\theta(x+r,y,z)\cdot\theta(x,y,z)\rangle/\langle\theta^2\rangle = 1-B_\theta(r/y)^{2/3} \quad \text{for} \quad y \gg r \gg \delta_K \tag{B9}$$

where $\delta_K = (\nu^3/\varepsilon)^{1/4}$ is the so-called Kolmogorov microscale (of dimension of length), $B_\theta = 3C_\theta\Gamma(1/3)/4a_2$, and Γ the Γ-function (cf. ref. [43]). The -1 power law (B8) together with law (B7) imply that

$$R_{\theta\theta}(r) = L_\theta = \text{const.} \quad \text{for} \quad y \ll r \ll \max(\delta, H) \tag{B10}$$

where $L_\theta = 1-G_\theta[1.5+\gamma+(3/2)\ln(C_\theta/G_\theta)]/a_2$; see ref. [14]. However, the estimate (B10) is rather crude; a more precise result obtained by performing the Fourier transform of the spectra $E_{\theta\theta}(k)$ consisting of two power ranges has the form

$$R_{\theta\theta}(r) = L_\theta - d_\theta \ln(r/y) \quad \text{for} \quad y \ll r \ll \max(\delta, H) \tag{B11}$$

where $d_\theta = G_\theta/a_2$; see ref. [43]. However at present there are no data to verify the theoretical results (B11).

TRANSFERT DE CHALEUR ET DE MASSE DANS DES COUCHES LIMITES AVEC GRADIENT DE PRESSION

Résumé—La structure d'un champ scalaire (température ou concentration d'un mélange passif) dans des couches limites en équilibre et avec gradient longitudinal de pression est étudiée par l'analyse dimensionnelle pour une région affine nommée "sous-couche à gradient" (où la distribution de température moyenne est décrite par une loi demi-puissance inverse) qui existe à la fois dans des écoulements accélérés et décélérés à gradient de pression. La loi d'écart de température, de forme spéciale, est valide dans la zone externe des couches limites à fort gradient. Les données expérimentales disponibles sur les profils de température dans les écoulements décélérés permettent de déterminer les constantes universelles et les fonctions entrant dans les relations théoriques et d'obtenir des formules d'interpolation décrivant le champ de température moyenne dans de telles conditions. En supposant qu'une couche de recouvrement existe où la loi d'écart et celle de sous-couche à gradient sont à la fois valides, on peut obtenir la loi universelle de transfert de chaleur et de masse. Les coefficients numériques de cette loi sont estimés pour les décélérations. Les formes de quelques caractéristiques statistiques de fluctuation de température sont comparées avec les données expérimentales disponibles.

WÄRME- UND STOFFÜBERGANG IN GRENZSCHICHTEN MIT EINEM DRUCKGRADIENTEN

Zusammenfassung—Die Struktur eines Skalarfeldes (Temperatur oder Konzentration eines nicht reagierenden Gemisches) in Grenzschichten mit gleitendem Gleichgewicht und mit Druckgradienten in Längsrichtung wird mit Hilfe der Dimensionsanalyse untersucht. In diesen Grenzschichten existiert ein selbstähnliches Gebiet, das als "gradient-sublayer" bezeichnet wird und dessen mittlere Temperatur dem inversen Wurzelgesetz gehorcht, und zwar für Wandströmungen mit positivem und negativen Druckgradienten. Darüberhinaus ist das Temperaturfehlergesetz in einer besonderen Form im äußeren Bereich von Grenzschichten mit starken Gradienten gültig. Die verfügbaren Versuchsdaten über Temperaturprofile in verzögerten Randströmungen erlauben es, universelle Konstanten und Funktionen zu bestimmen, welche in die theoretischen Beziehungen eingehen. Zudem werden Interpolationsformeln zur Beschreibung des mittleren Temperaturfeldes für diese Bedingungen ermittelt. Unter der Annahme, daß eine Übergangsschicht existiert, in der sowohl das Fehlergesetz als auch das "gradient-sublayer"-Gesetz gilt, ergibt sich ein verallgemeinertes Gesetz für die Wärme- und Stoffübertragung. Die numerischen Koeffizienten für dieses Gesetz werden für den Fall einer Strömung mit verzögerten Druckgradienten bestimmt. Es werden einige statistische Eigenschaften der Temperaturfluktuationen (insbesondere die mehrdimensionale Wahrscheinlichkeitsdichte, die Spektren und Momente) in der "gradient-sublayer"-Schicht mit Hilfe der Dimensionsanalyse bestimmt und abschließend mit verfügbaren experimentellen Daten verglichen.

ТЕПЛО- И МАССОПЕРЕНОС В ГРАДЕНТНОМ ПОГРАНИЧНОМ СЛОЕ

Аннотация—С помощью комбинации методов размерности и асимптотических разложений исследована структура осредненного скалярного поля (температуры или концентрации пассивной примеси) в турбулентных пограничных слоях с продольным градиентом давления, ускоряющим или замедлющим поток, в условиях справедливости гипотезы локальной равновесности течения. Показано, что наличие дополнительного параметра—продольного градиента давления—приводит к появлению в пограничном слое области, распределение температуры в которой описывается "обратным законом квадратного корня". В соответствии с предсказаниями теории этот закон оказывается справедливым как для замедляющихся, так и ускоряющихся потоков. При этом во внешней зоне пограничного слоя, развивающегося в условиях существенного продольного градиента любого знака, справедлив своеобразный закон дефекта температуры. Основываясь на имеющихся экспериментальных данных о профилях температуры в замедляющихся пристенных течениях удается определить значения универсальных констант и функций, входящих в полученные общие соотношения, и построить интерполяционные зависимости, позволяющие добиться вполне удовлетворительного описания распределения температуры в этих условиях. Основываясь на предположении о существовании области перекрытия закона дефекта и градиентного закона распределения температуры (т.е. предполагая существование области сращивания полученных асимптотических разложений) получен универсальный закон тепломассопереноса в градиентаных потоках. Для случая тормозящего градиента давления определены значения коэффициентов, входящих в этот закон. На основании следствий из анализа размерностей, касающихся общего вида многомерной плотности вероятности знажений пульсаций температуры, предсказано и проверено сравнение с экспериментом поведение некоторых статистических характеристик температурных пульсаций в градиентном подслое.